ISSN 0007-2621

No. 2 — 1981

published quarterly

Technical Review

To Advance Techniques in Acoustical, Electrical and Mechanical Measurement

Acoustic Emission Source Location

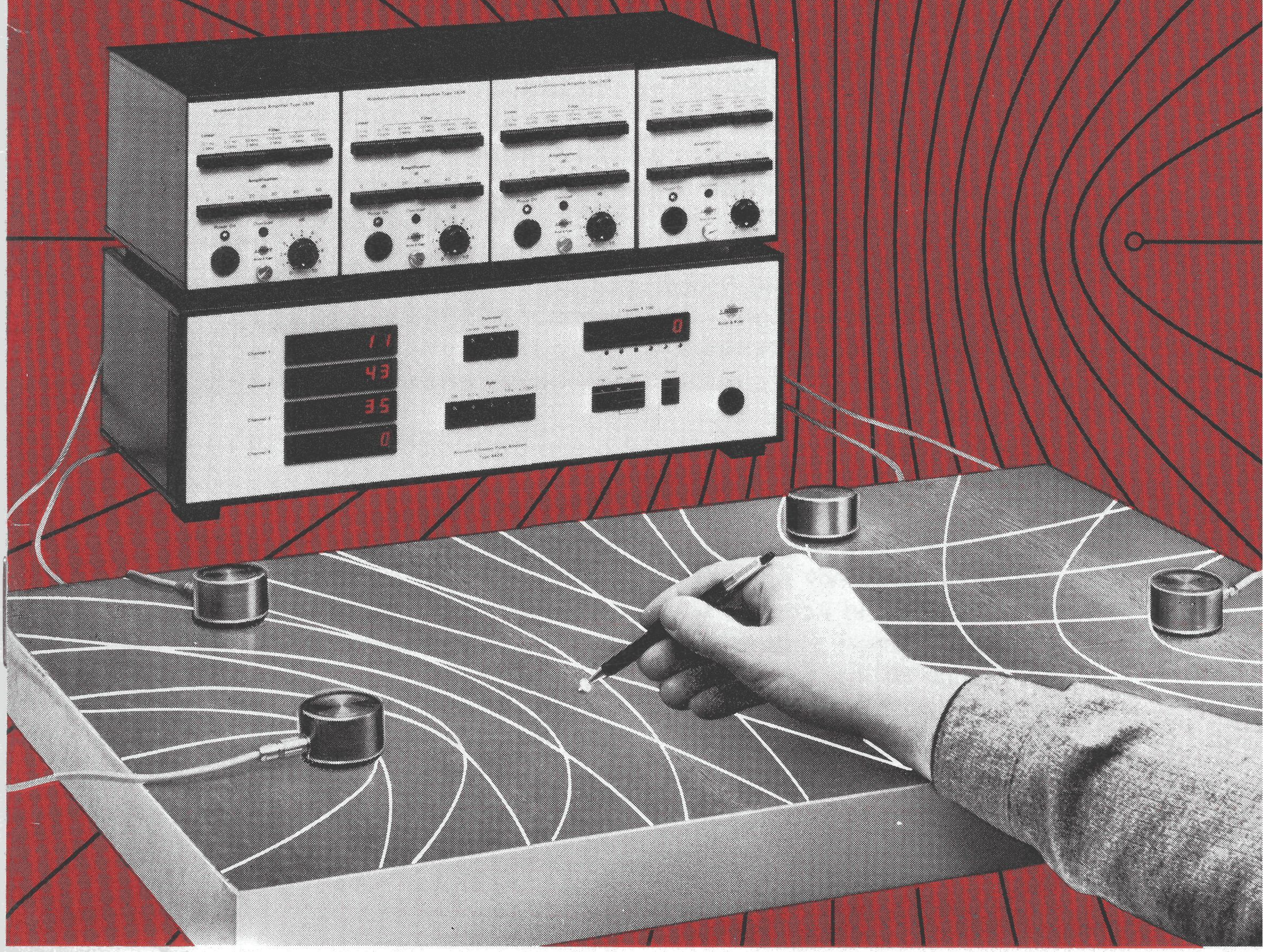

Brüel & Kjær

PREVIOUSLY ISSUED NUMBERS OF BRÜEL & KJÆR TECHNICAL REVIEW

1-1981 The Fundamentals of Industrial Balancing Machines and their Applications

4-1980 Selection and Use of Microphones for Engine and Aircraft Noise Measurements.

3-1980 Power Based Measurements of Sound Insulation.
Acoustical Measurement of Auditory Tube Opening.

2-1980 Zoom-FFT.

1-1980 Luminance Contrast Measurement.

4-1979 Prepolarized Condenser Microphones for Measurement Purposes.
Impulse Analysis using a Real-Time Digital Filter Analyzer.

3-1979 The Rationale of Dynamic Balancing by Vibration Measurements.
Interfacing Level Recorder Type 2306 to a Digital Computer.

2-1979 Acoustic Emission.

1-1979 The Discrete Fourier Transform and FFT Analyzers.

4-1978 Reverberation Process at Low Frequencies.

3-1978 The Enigma of Sound Power Measurements at Low Frequencies.

2-1978 The Application of the Narrow Band Spectrum Analyzer Type 2031 to the Analysis of Transient and Cyclic Phenomena.
Measurement of Effective Bandwidth of Filters.

1-1978 Digital Filters and FFT Technique in Real-time Analysis.

4-1977 General Accuracy of Sound Level Meter Measurements.
Low Impedance Microphone Calibrator and its Advantages.

3-1977 Condenser Microphones used as Sound Sources.

2-1977 Automated Measurements of Reverberation Time using the Digital Frequency Analyzer Type 2131.
Measurement of Elastic Modulus and Loss Factor of PVC at High Frequencies.

1-1977 Digital Filters in Acoustic Analysis Systems.
An Objective Comparison of Analog and Digital Methods of Real Time Frequency Analysis.

4-1976 An Easy and Accurate Method of Sound Power Measurements.
Measurement of Sound Absorption of rooms using a Reference Sound Source.

3-1976 Registration of Voice Quality.
Acoustic Response Measurements and Standards for Motion-Picture Theatres.

2-1976 Free-Field Response of Sound Level Meters.
High Frequency Testing of Gramophone Cartridges using an Accelerometer.

1-1976 Do We Measure Damaging Noise Correctly?

(Continued on cover page 3)

TECHNICAL REVIEW

No. 2 — 1981

Contents

ACOUSTIC EMISSION SOURCE LOCATION IN THEORY AND IN PRACTICE

by

H. J. Rindorf, M.Sc.

ABSTRACT

One of the potentially most useful features of acoustic emission monitoring is the source location capability. Various algorithms exist to accommodate mathematically simple structures and these may be combined to cover more complex geometries. This article describes the method of source location based on the relative arrival times of an AE signal at various transducers and examines factors which give rise to errors even in simple geometries. In particular, the wave velocity and measurement of arrival time problems are discussed. Expected magnitudes of errors can be developed theoretically and verified by experiment. Source location accuracy can be determined graphically as a complex pattern which is independent of the algorithm used. Consideration of these factors provides guidelines for optimum transducer arrays and measurement technique.

SOMMAIRE

L'une des caractéristiques potentiellement plus utiles de la surveillance de l'émission acoustique est la possibilité de localiser la source. Divers algorithmes existent pour le traitement de structures mathématiquement simples, et ils peuvent être combinés pour des géométries plus complexes. Cet article décrit la méthode de localisation de la source basée sur les temps d'arrivée relatifs de signaux d'EA aux divers capteurs, et étudie les facteurs qui créent des erreurs même pour des géométries simples. Les problèmes de vitesse de l'onde et de mesure des temps d'arrivée sont plus particulièrement discutés. La valeur des erreurs attendues peut être développée théoriquement, et vérifiée par expérience. La précision de la localisation de la source peut être donnée par un réseau complexe indépendant de l'algorithme utilisé. Les considérations sur ces facteurs fournissent les grandes lignes pour optimiser les réseaux de capteurs et les techniques de mesure.

ZUSAMMENFASSUNG

Die Möglichkeit der Ortung ist eine der vorteilhaftesten Merkmale in der Überwachung der Schallemision (SE). Es existieren verschiedene Algorithmen, die die mathematisch einfach zu

beschreibenden Strukturen behandeln und die sich miteinander kombinieren lassen, wenn kompliziertere Strukturen überwacht werden. Dieser Artikel beschreibt eine Ortungsmethode, die auf der relativen Laufzeitdifferenz der SE-Signale von verschiedenen Aufnehmern beruht und es werden Fehlermöglichkeiten untersucht. Speziell werden Probleme bei der Bestimmung der Fortpflanzungsgeschwindigkeit der Welle und der Messung der Ankuftszeit des SE-Signals untersucht. Die Größenordnung der zu erwartenden Fehler läßt sich theorethisch bestimmen und im Experiment bestätigen. Die Ortungsgenauigkeit läßt sich graphisch als ein komplexes Muster darstellen und ist vom benutzten Algorithmus unabhängig. Aufgrund dieser Faktoren läßt sich die optimale Anordnung der Aufnehmer sowie die optimale Meßtechnik ermitteln.

Introduction

When a material or structure is loaded, internally stored energy may be spontaneously released in a form of acoustic energy called a stress wave. The energy release occurs when irreversible deformation processes or changes in the atomic ordering are active within a material and the resulting stress wave propagates through the material to the structure surface where it may be detected using sensitive piezoelectric transducers. This phenomenon, which is called Acoustic Emission or stress wave emission, has found practical application in the past two decades as a non-destructive testing (NDT) technique [1]. Acoustic emission (AE) differs from other NDT techniques in that it is an active method able to detect when a flaw or crack occurs and in some cases where it occurs.

In using AE to monitor and detect various defects it is often required to locate the source of emission. In general, a manufacturer will examine a structure to ensure that it complies with specifications, measure physical dimensions and check the welds and joints. These checks may be carried out using static methods of inspection i.e. the structure is examined on its own by visual inspection, dye penetrants and similar "decorative" methods, or other established NDT techniques. During a subsequent test where the structure is subjected to a proof or service load, and on into service life, active defects may be detected and located using AE. One or more of the static inspection methods can then be applied for a detailed examination of the defect and its causes. The source location capability is therefore one of the most useful aspects of acoustic emission monitoring. Several transducers may be used to cover large areas of a structure and identify the active regions, limited access to the structure is sufficient, and the method is not restricted to surface flaws or by defect size. Although the mathematics of source location is fairly involved and the location accuracy is limited, these factors are not prohibitive.

Some reports [2], [3], [4], [5] indicate remarkable success in locating defects using AE. Others, however, rather disappointingly report that even after

large amounts of data were collected, it was either not possible to calculate the position of the defect or that the location accuracy was much less than expected.

Principle Of Source Location

AE signals can be broadly divided into two classes: a) burst type emission which is detected as decaying sinusoids and b) continuous emission (resembling white noise). AE source location is based on measurements of the relative arrival times of an AE signal at several transducers and is therefore confined to applications where the sources generate burst type signals. Furthermore, the wave velocity is normally assumed to be uniform throughout the medium.

In the 1-dimensional case, where the source is known to lie somewhere along a straight line between a pair of transducers, a difference in measured arrival times at the transducers uniquely determines the source location.

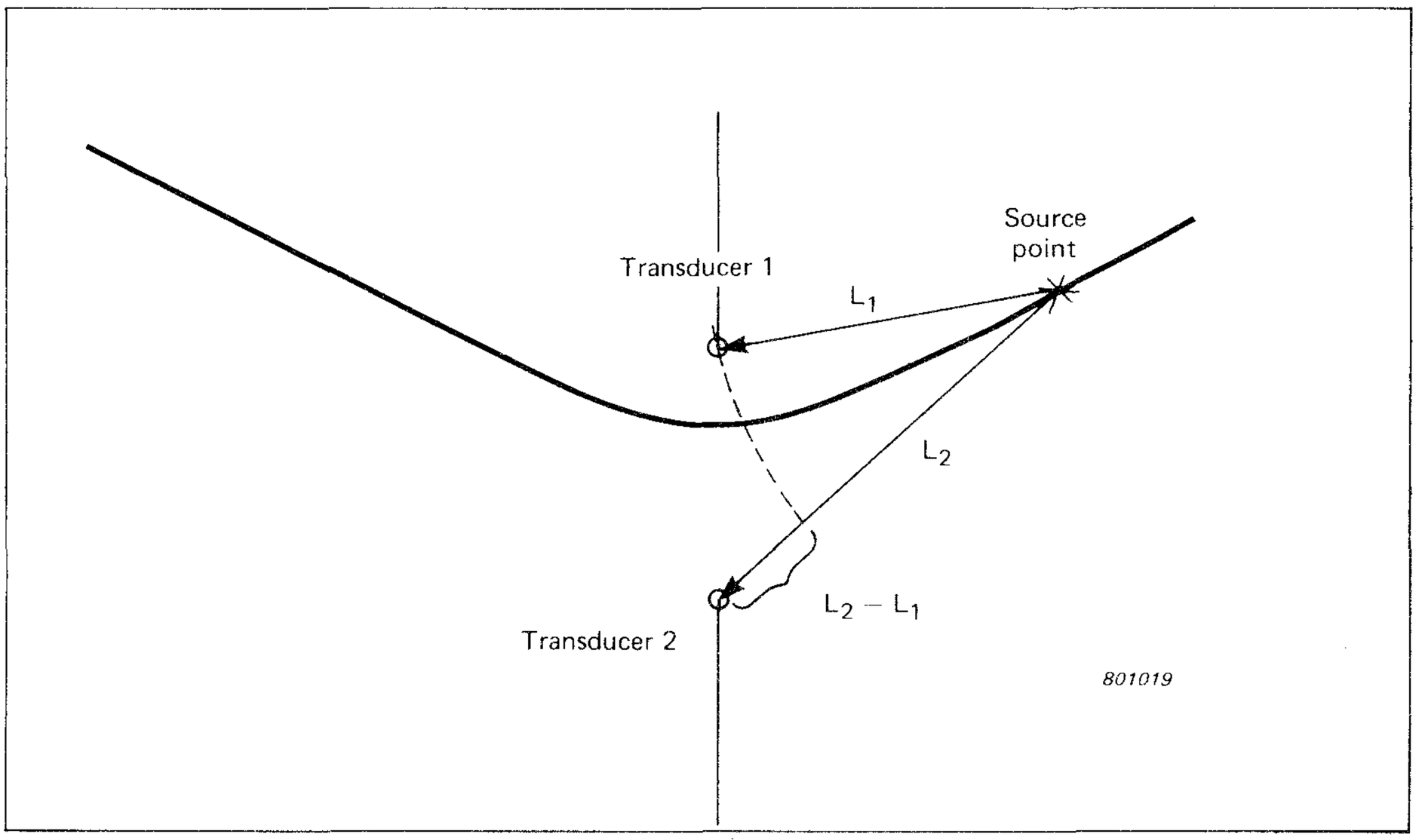

Fig. 1. The AE wave is detected by the two transducers at different times. A signal from any point on the hyperbola will result in the same measured time delay

In the 2-dimensional case shown in Fig. 1, where the source is known to lie at a point in a plane, the difference in distance travelled by the wave to a pair of transducers can be calculated from the measured time difference:

$$\delta = \Delta t \cdot v \qquad (1)$$

where δ is the path difference, v is the wave velocity and Δt is the measured time delay. The same path difference, δ, is obtained if the source lies at any point along a hyperbola with the transducers at the focii. Using additional transducers the coordinates of the source can be determined from the intersection of hyperbolae defined by the measured time differences at other transducer pairs. In general, a number of N transducers will yield N–1 time differences and coordinates. Thus the minimum number of transducers required is two for linear location, three for a plane and four for a volume.

Ambiguity

Ambiguous solutions sometimes arise when the minimum number of trans-

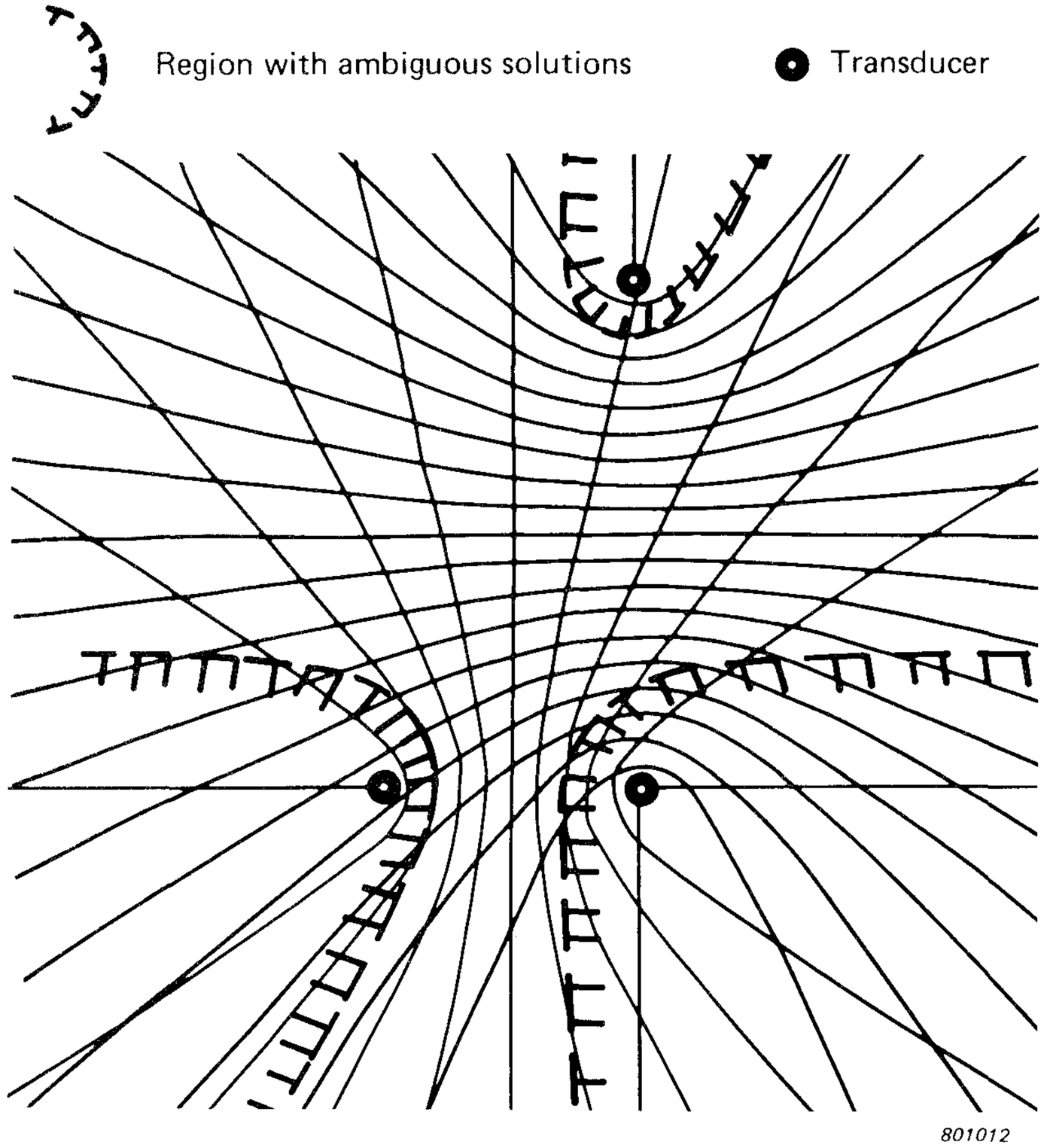

Fig. 2. Regions with ambiguous solutions exist near and "behind" each transducer

ducers are used. In the region close to and "behind" each transducer there is a certain area in which twin solutions occur. This is shown in Fig. 2. Both solutions are physically meaningful and in order to resolve the ambiguity additiona! information must be collected. This can be done by measuring the time delay to an extra transducer and comparing it with the calculated value for the source location.

Numerical Solution

The algorithm used to calculate the source location from the collected data may be based on several methods. Numerical solutions can be calculated using iterative methods, tables, or a direct mathematical solution. Tables have a limited resolution and neither tables nor iterative methods can generally be used to correctly resolve situations where ambiguous solutions occur. Convenient and exact mathematical algorithms for a plane and spherical surface have been published by Tobias [6] and Asty [7] respectively, and an iterative algorithm for source location in three dimensions has been developed by Blake et al. [5]. Tobias [6] also discusses ambiguity and spatial resolution for three different transducer arrays.

A source location program for a HP 41-C calculator is given in Appendix B. The program, which is based on the algorithm given in Appendix A, calculates the source position from the measured arrival times at three transducers arranged in a right-angled triangular array.

Measurement Results

In discussions and in published literature it is often reported that AE source location experiments have produced poor results. Some researchers informally report that only 2 %, or less, of the detected events result in an accurate source location or that the accuracy was very much less than that obtained using calibration methods prior to the test.

Fig. 3. shows an example from a carefully controlled experiment where AE was expected and confirmed but the source location was less successful. Obata & Bentley [8] conducted a series of tests on a 1 m diameter cylindrical pressure vessel of length 4,3 m in which a 400 mm axial defect was cut to a depth of 60 % of the wall thickness. The vessel was pressurized several times and finally failed at 1480 psi. In addition to monitoring the total AE count rate, the relative arrival times at diagonally opposite transducers in a square array were plotted directly as shown in Fig. 3. During calibration both ends of the artificial defect were excited and the "source" positions were successfully determined. When the vessel was pressurized, however, the

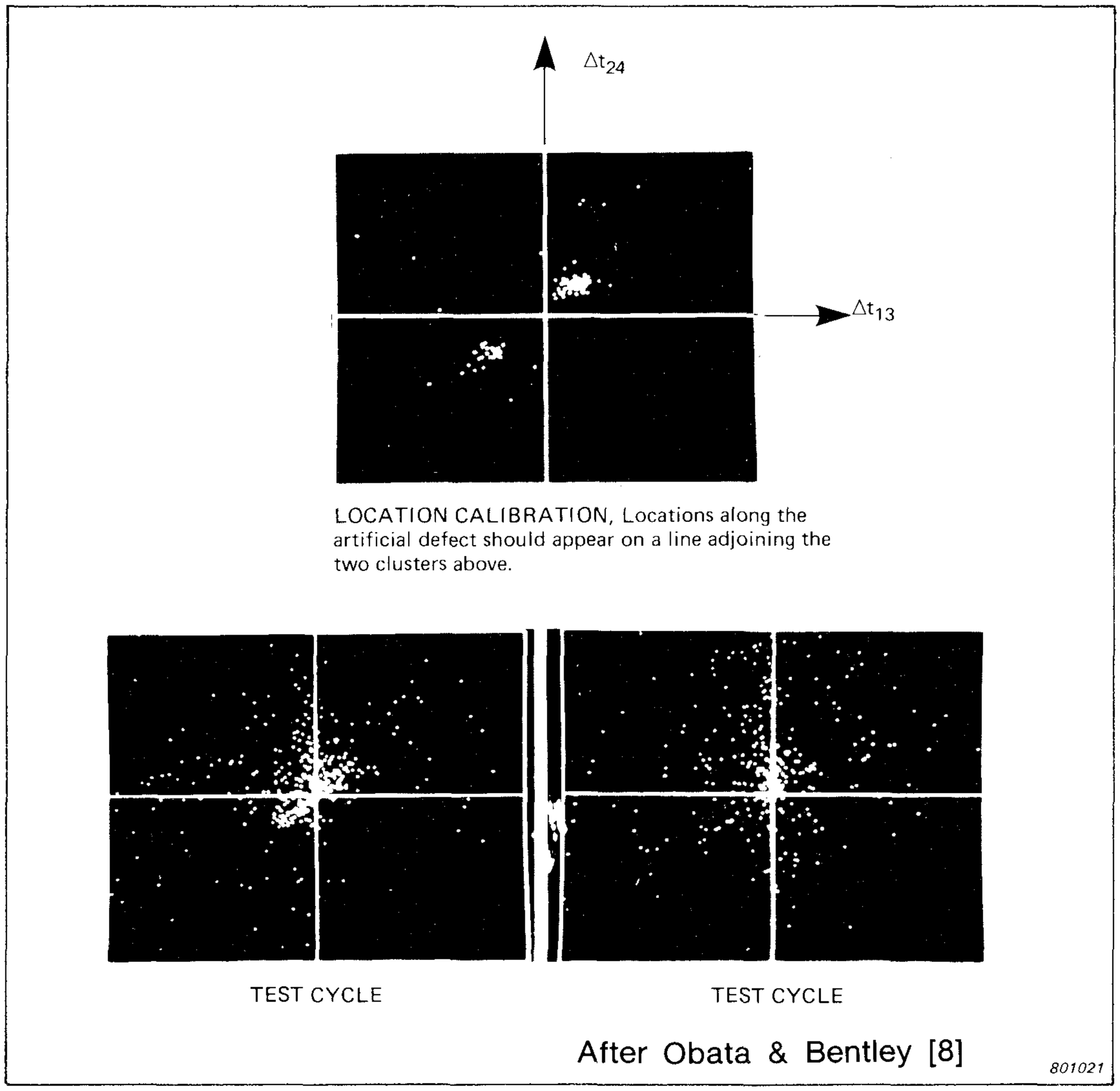

Fig. 3. Example of a test where the time delays measured by a square array of transducers were plotted directly. Location calibration using an artificial source was accurate. Location of acoustic emission during subsequent test cycles was more scattered

location of real AE sources showed considerable scattering. The results indicate a higher density of source locations around the artificial defect but there is wider spreading than was expected in this simple case.

Possible Sources Of Error

The source location calculation requires knowledge of the structure geometry, the positions of the transducers, the wave velocity and the measured relative arrival times. The extent to which these factors influence the resulting accuracy is now discussed.

a) Structure Geometry

The structure geometry is assumed to be fairly simple, i.e. the straight path travelled by the wave from the source epicentre (the projection of the source location onto the structure surface) to the transducers is unbroken. This assumption is made in the following discussion.

b) Transducer Positioning

The location accuracy is inherently limited by the active surface area of the transducer. For many transducer types the effective diameter is approximately 20 mm, although some types are available with an active diameter down to 3 mm (e.g. B & K Broad-Band Transducer Type 8312). In addition, the arrangement of the transducers in an array determines the accuracy of location (the spatial resolution) and the extent of regions where ambiguous solutions may occur.

c) Wave Velocity

The propagation of acoustic waves in solid media is a complex problem. In

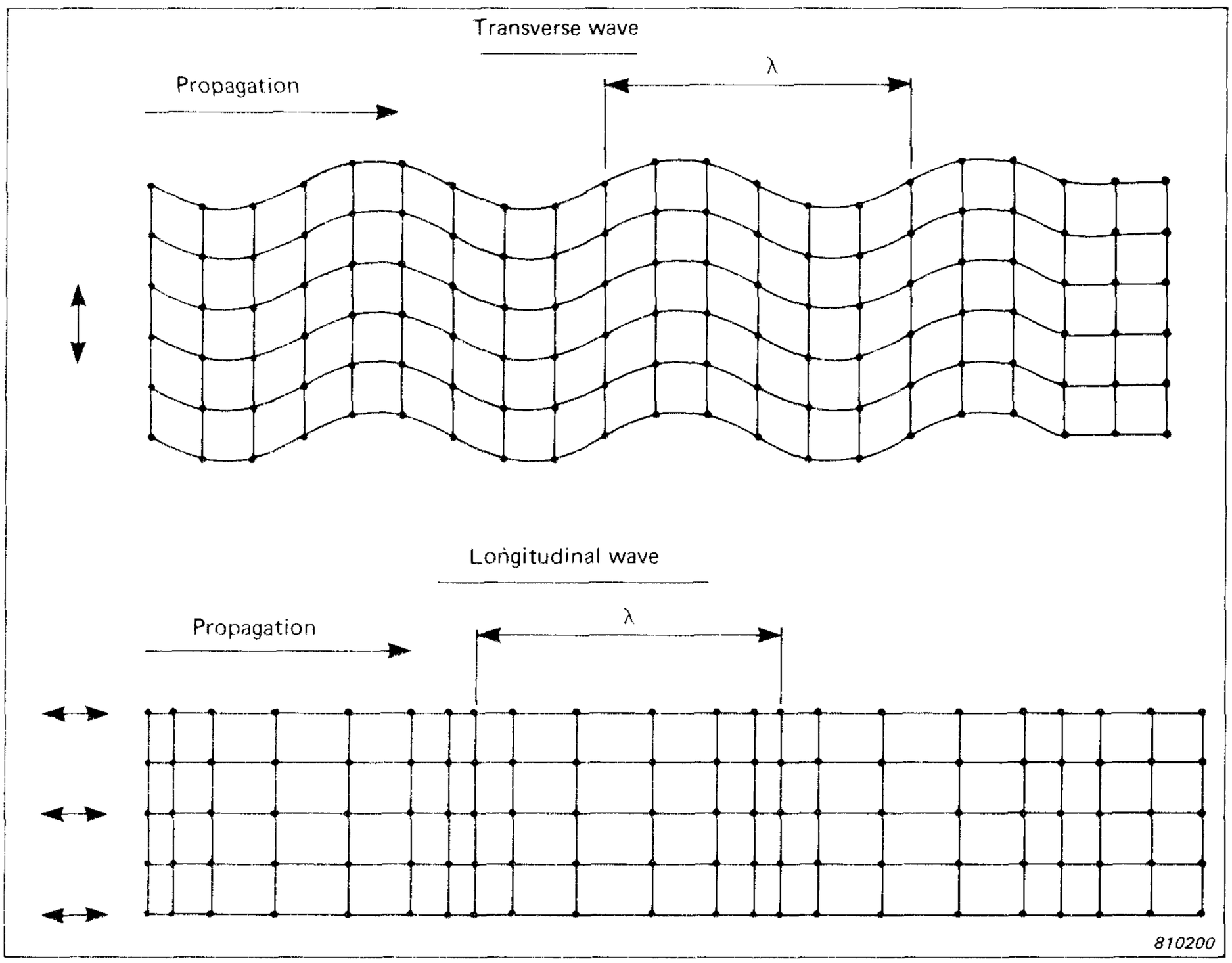

Fig. 4. The two basic wave modes in a solid

an infinite medium elastic waves propagate in two basic forms, as longitudinal waves and transverse waves, each with a characteristic velocity which can be calculated from the density and elastic constants of the solid [9]. The particle motion in a longitudinal wave is parallel to the wave propagation direction and consists of localized compression and rarefaction of the medium. Transverse waves, which do not propagate in gasses or liquids, are characterized by particle motion which is perpendicular to the wave propagation direction. These two basic waveforms are shown in Fig. 4.

If a surface or boundary is introduced, i.e. in a half-space, the longitudinal and transverse waves which propagate in the bulk of the material combine in the region close to the surface; a compression produces a transverse displacement in accordance with the Poisson's ratio of the material so that the overall particle motion is neither purely longitudinal nor purely transverse. This type of surface wave, shown in Fig. 5, is called a Rayleigh wave. The characteristic velocity of Rayleigh waves can also be calculated from the physical constants of the material and is generally less than that for either of the bulk waveforms. In a medium bounded by two surfaces, i.e. a plate, the waveforms couple at the surfaces to produce the two basic modes shown in Fig. 6. These are called the symmetric, s_0, and asymmetric, a_0, wave modes; the particle displacement is either longitudinal (s_0) or transverse (a_0) in the plate centre line. As wavelengths become shorter relative to the plate thickness, higher order symmetric and asymmetric modes are

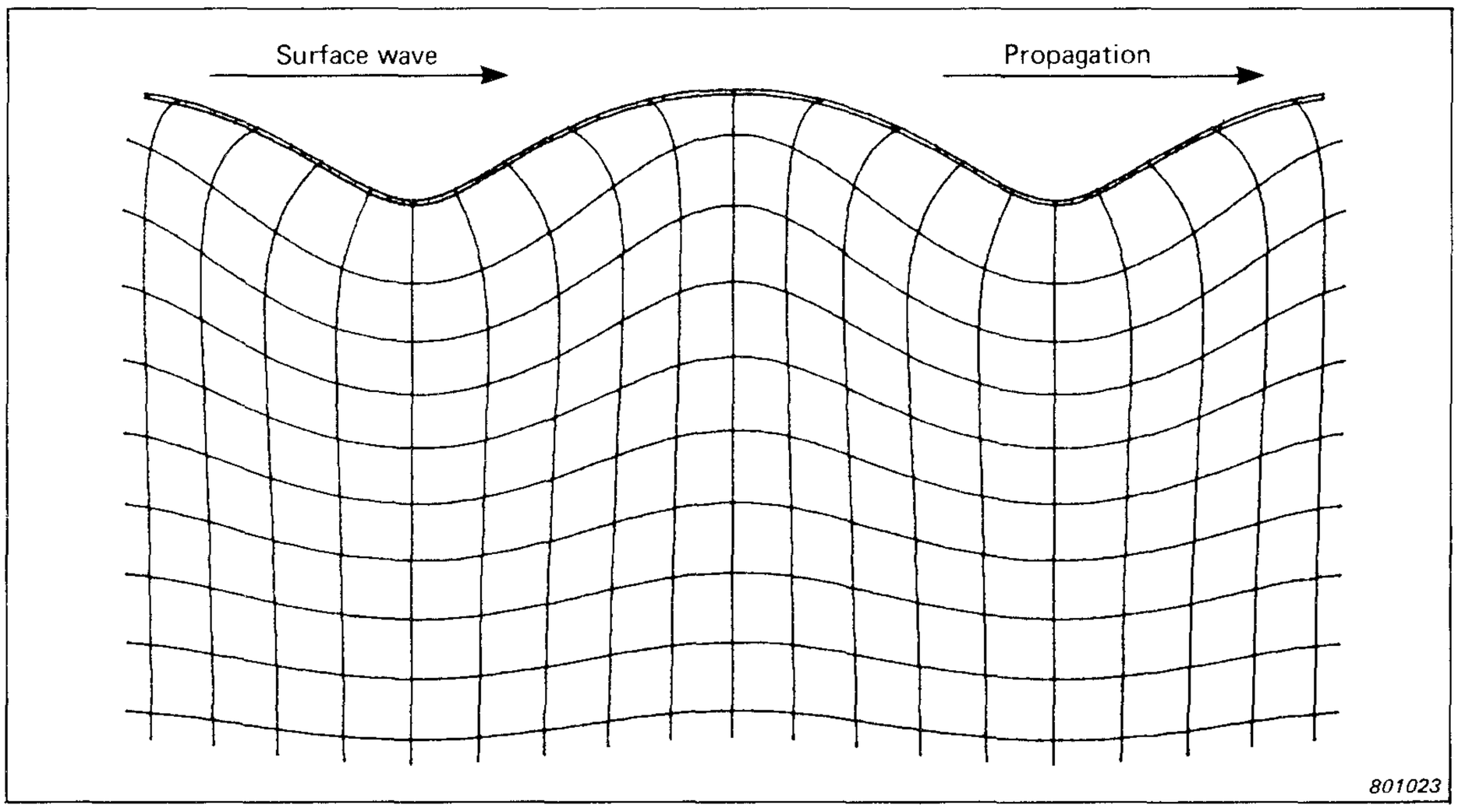

Fig. 5. The particle motion in a surface wave is neither purely longitudinal nor purely transverse

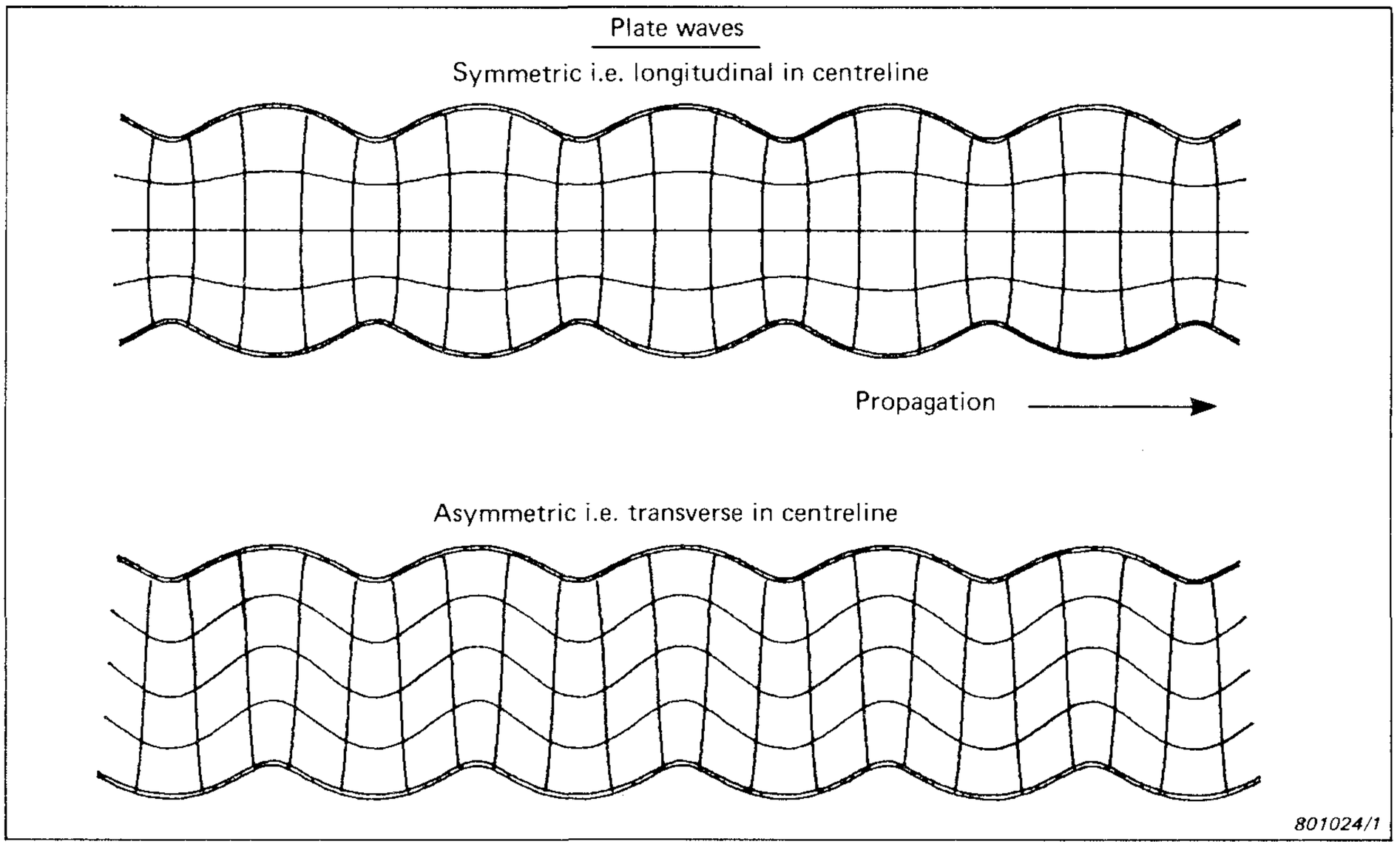

Fig. 6. The two basic wave modes in a plate

possible, each with a characteristic group velocity dependent on the plate thickness [10], as shown in Fig. 7. For a fixed plate thickness this causes dispersion i.e. wave components of different frequencies will travel at different speeds and an impulse signal will be spread out in time.

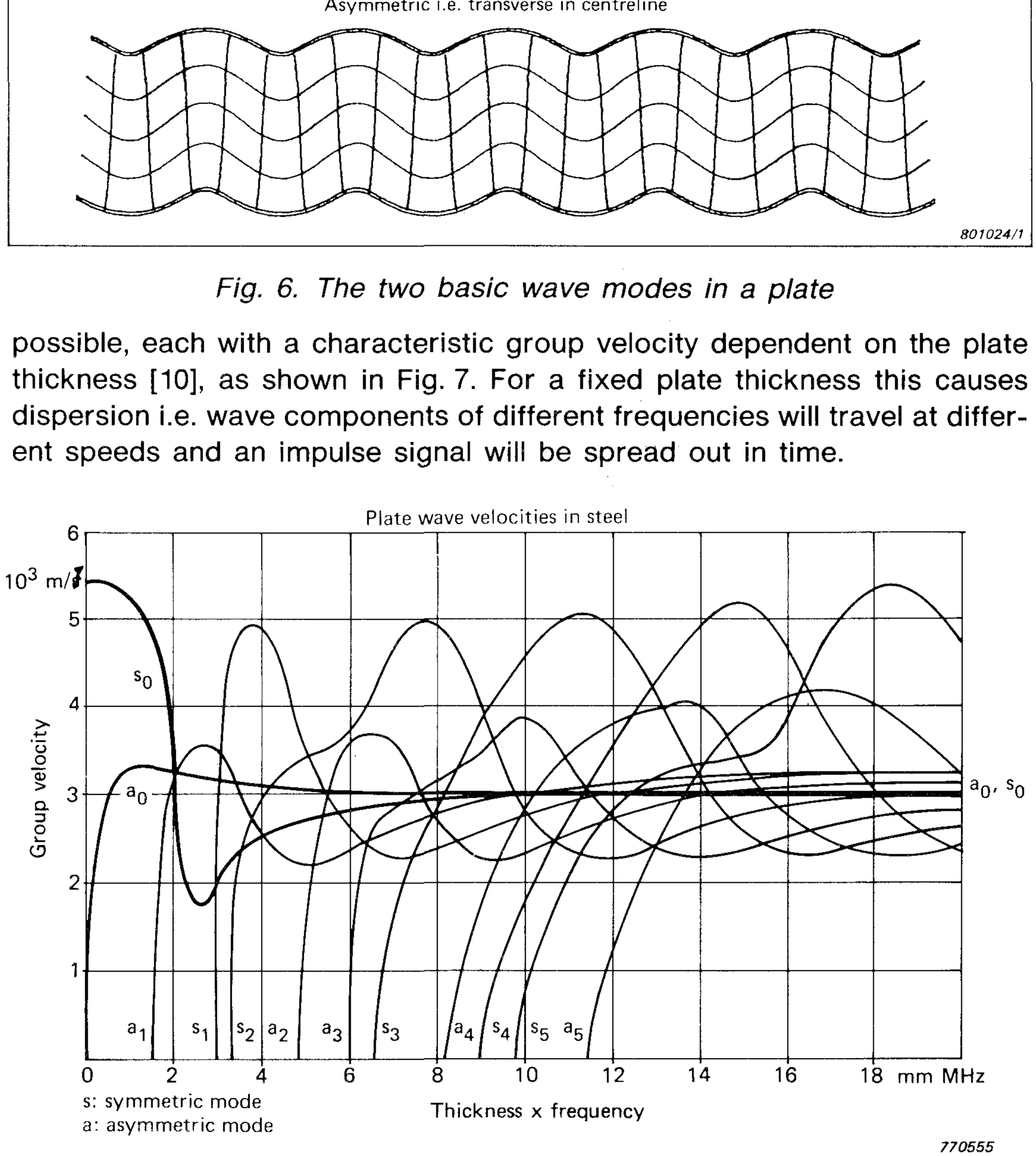

Fig. 7. Surface wave modes in a steel plate

Various sources generate different combinations of modes which may gradually change due to attenuation in the medium. When a pulse train crosses a boundary such as a weld or a change in plate thickness, mode conversion occurs. Although a transducer which is placed near such a boundary can be used for source location on either side, it may be necessary to consider different velocities for each plate section.

At the pick-up point some separation of the wave modes can be effected using the frequency bandwidth of the transducer and amplifying system. Therefore, matching the frequency range and the plate thickness may affect the effective wave velocity considerably. Incorrect assumptions of the frequency and plate thickness may lead to velocity values of the order of 50 % of the correct figure.

d) Arrival Time

Errors incurred in the measurement of arrival times at the transducers are primarily due to the dispersion phenomenon. Secondary problems occur due to phase uncertainty and superposition of multiple events. These factors are discussed in the following.

1. Dispersion Phenomenon:

To illustrate the difficulties in determining the arrival time, experiments were carried out on two aluminium plates of different thicknesses (50 mm and 6 mm). The plates were excited by breaking a 0,5 mm pencil lead on the plate surface. This very repeatable signal results in a close physical approximation to a step function force. (A fuller discussion of this source is given in Appendix C.) By placing AE transducers successively on both sides of the plates at various distances from the point of excitation, the plate dispersion phenomenon in the near ($<$ 10 plate thicknesses) and far acoustic fields can be illustrated. The experiments were carried out using the B & K Broad-Band Transducer Type 8312 and Resonance Transducers Types 8313 (resonance at 200 kHz) and 8314 (resonance at 800 kHz). Frequency response curves for the three transducers are shown in Fig. 8. An amplifying bandwidth of 0,1 Hz to 2 MHz for transducer Type 8313 and 10 kHz to 2 MHz for transducers Types 8312 and 8314 was used. The results were recorded on a transient recorder with 20 MHz sampling rate and memory capacity of 100 μs. In practical AE measurements a narrower bandwidth (e.g. high-pass from 100 kHz) would normally be used. A wider bandwidth was chosen for this investigation to obtain the maximum amount of information from the experiments.

Results in the near acoustic field (Figs. 9 to 11) show a marked difference between corresponding pulse trains recorded on the two sides of the plate.

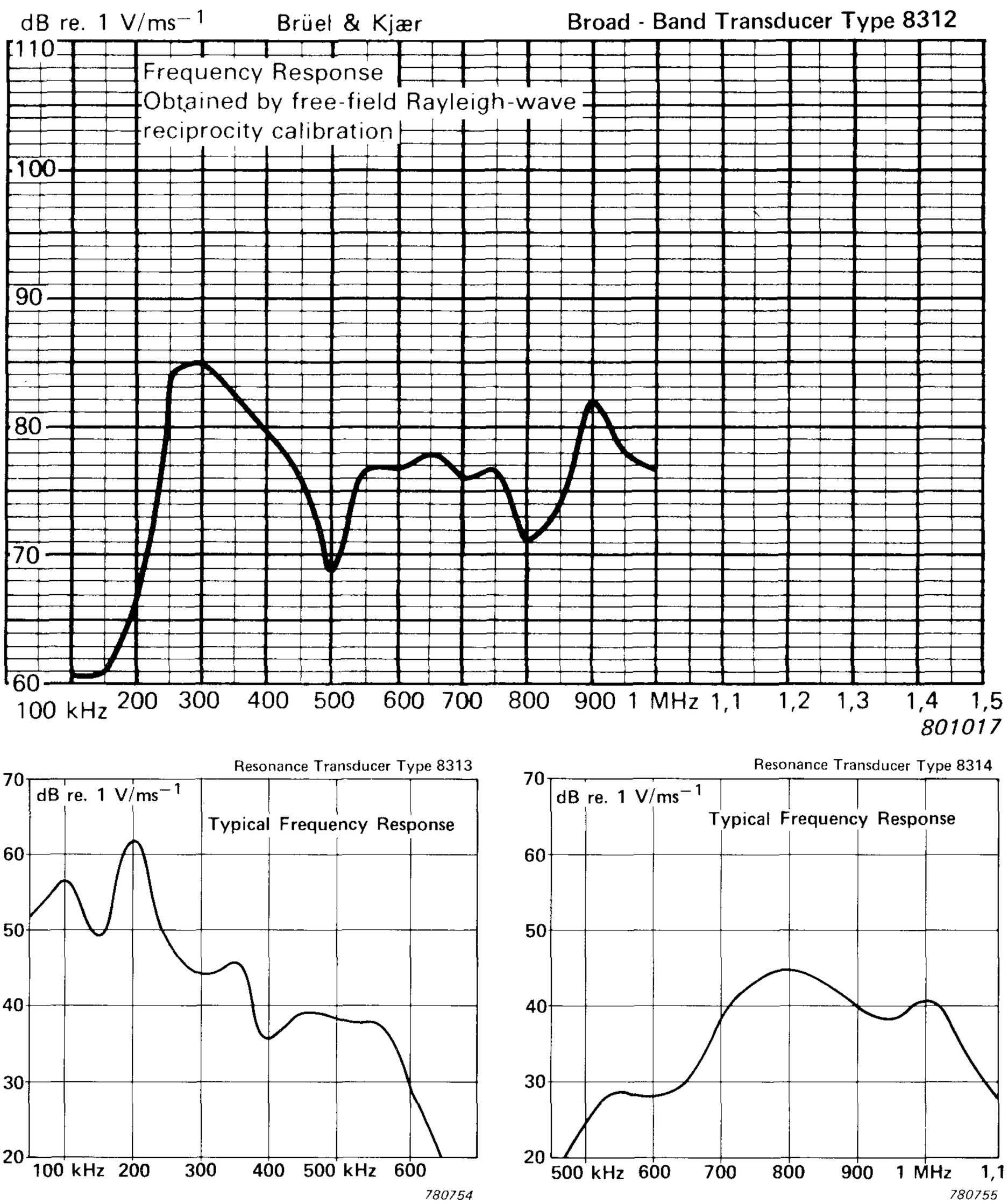

Fig. 8. Frequency response of Transducers Types 8312, 8313 and 8314

A distinctive surface wave (Rayleigh wave) is dominant on the same side as the source but absent on the opposite side of the plate. This effect is most prominent with transducer types 8312 and 8314 (Figs. 9 and 11). Apparently the surface wave pulse content is dominated by a higher level of high frequency components thus exciting the 800 kHz transducer more than the 200 kHz transducer.

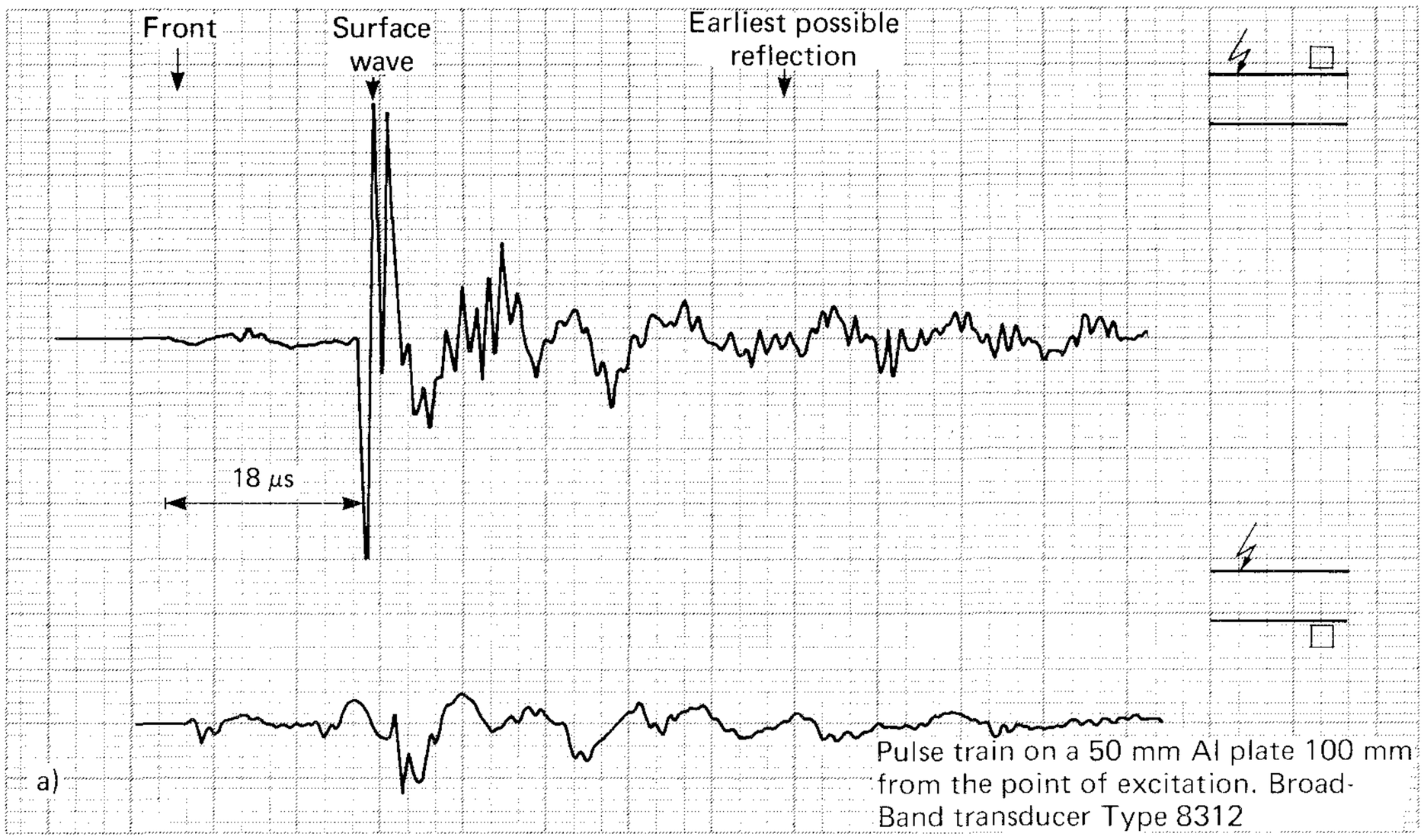

Fig. 9. Pulse trains recorded in the near acoustic field using Broad-Band Transducer Type 8312. Each figure shows the pulse detected on opposite sides of the plate at a distance of
a*) 100 mm from the point of excitation*
b) 200 mm from the point of excitation

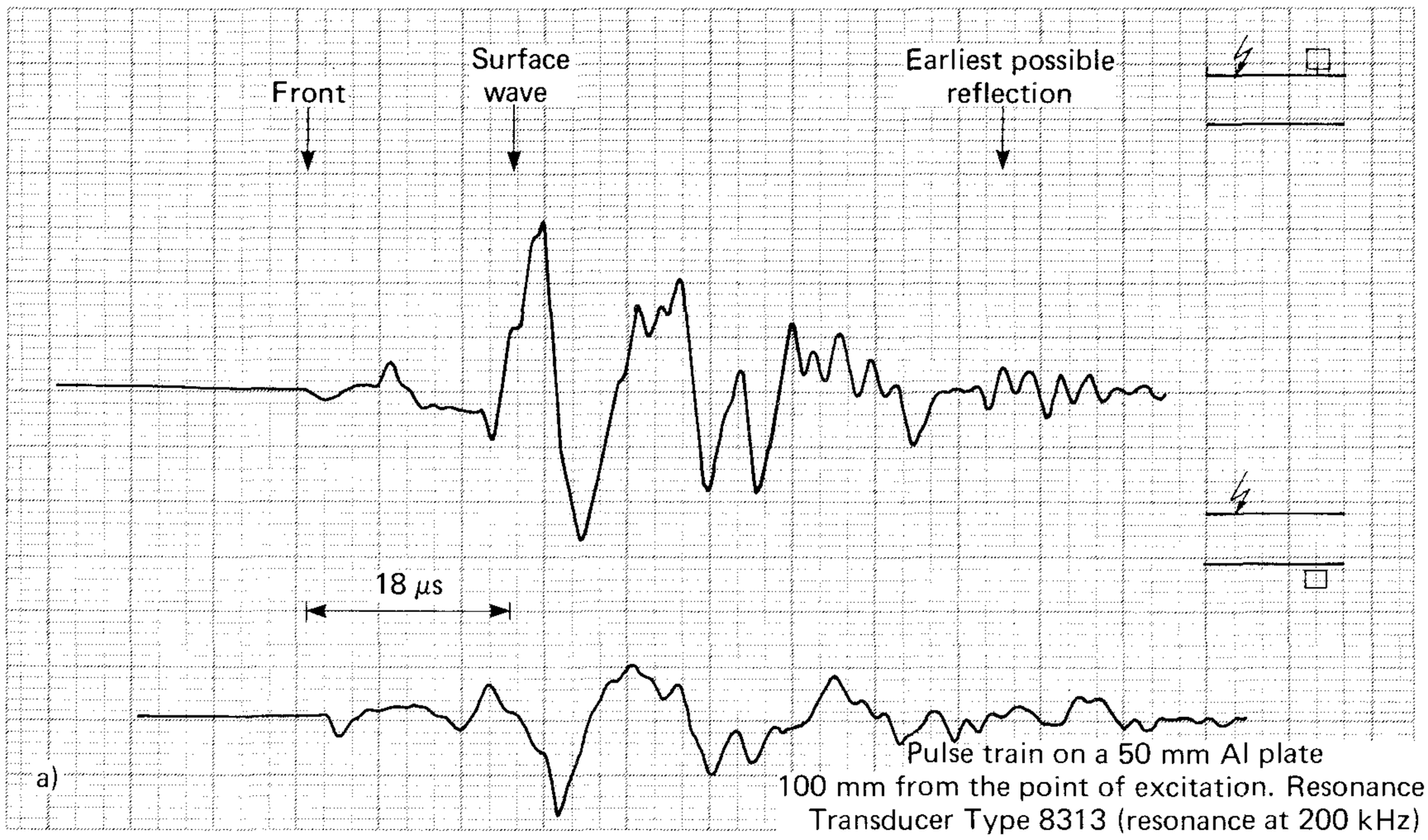

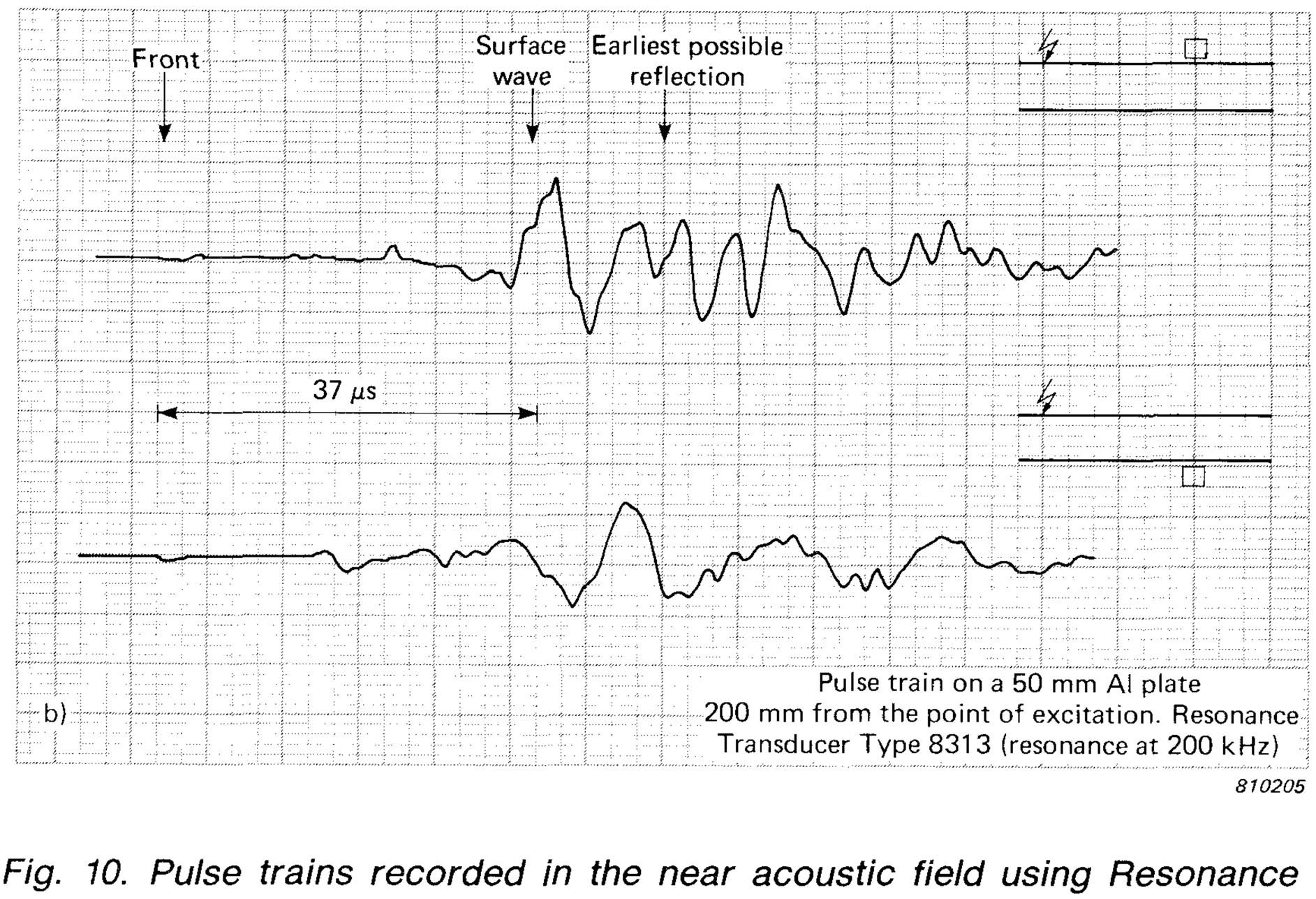

Fig. 10. Pulse trains recorded in the near acoustic field using Resonance Transducer Type 8313. Each figure shows the pulse train detected on opposite sides of the plate at a distance of
a) 100 mm from the point of excitation
b) 200 mm from the point of excitation

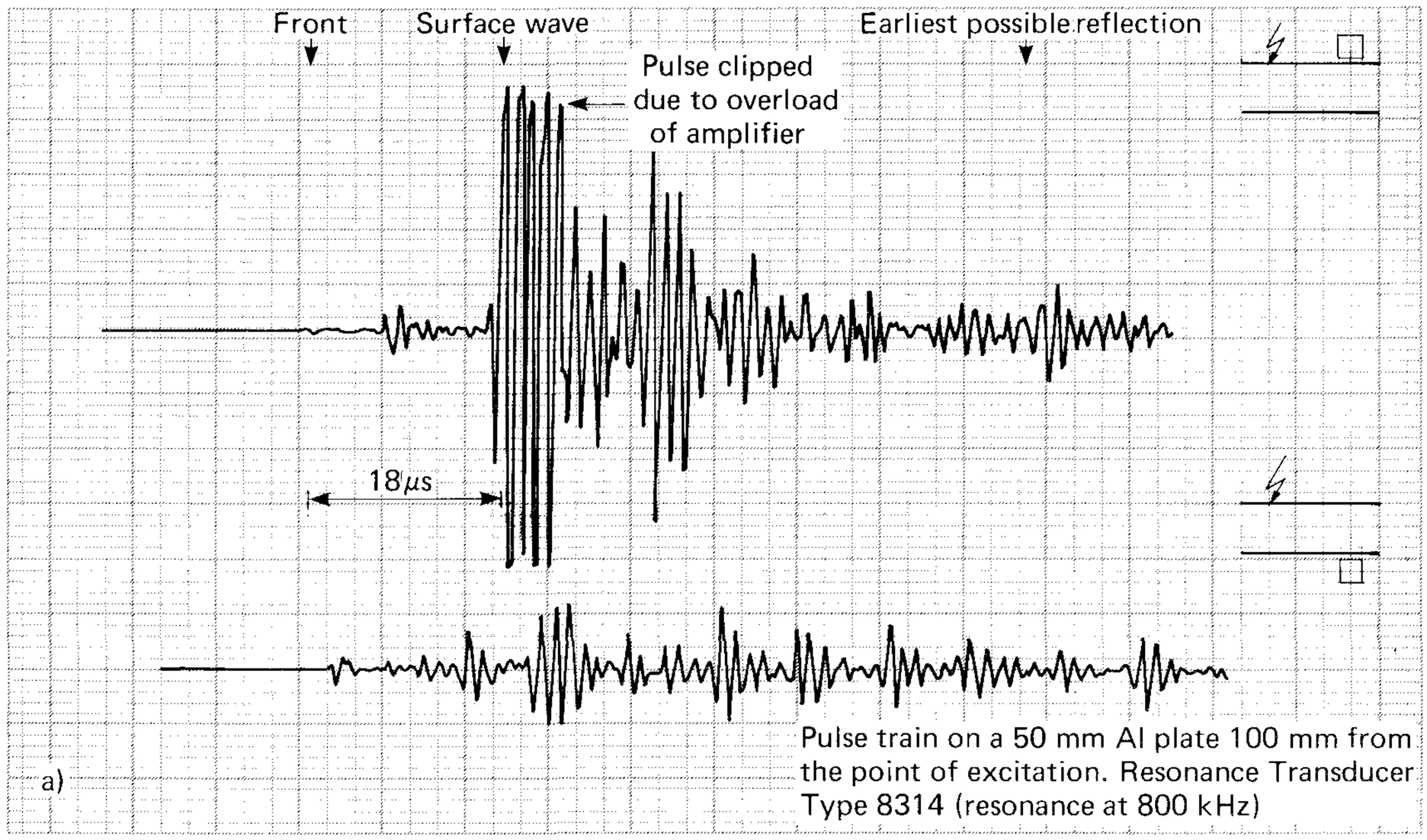

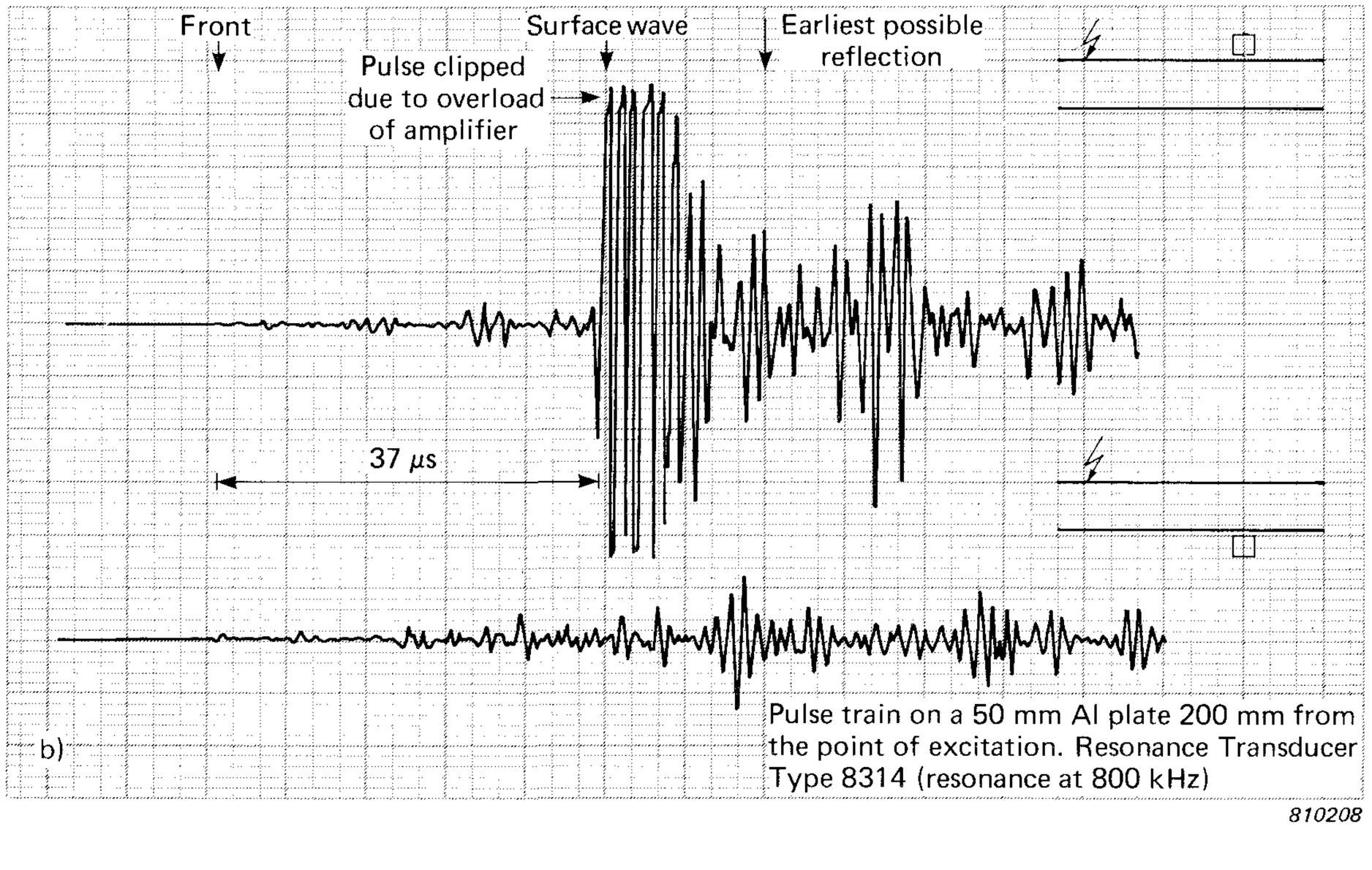

Fig. 11. Pulse trains recorded in the near acoustic field using Resonance Transducer Type 8314. Each figure shows the pulse train detected on opposite sides of the plate at a distance of
a) 100 mm from the point of excitation
b) 200 mm from the point of excitation

Based on the assumption that the peak amplitude of the signal indicates the passage of the Rayleigh wave shown in the figures, it is possible to calculate the time elapsed since the pencil lead was broken using the Rayleigh wave velocity for the plate and the distance from the source to the transducer. Since the velocity of longitudinal waves is greater than that of either transverse or Rayleigh waves, the arrival time of the earliest possible wave can then be calculated using the longitudinal wave velocity. The difference between the arrival times of the Rayleigh wave and the longitudinal wave is calculated to be 18 μs and 36 μs for a distance of 100 mm and 200 mm from the source to the transducer respectively. This permits calibration of the time scale, marking the "front" or leading pulse as a longitudinal wave. In the interval between the arrival of the fastest (longitudinal) wave and the Rayleigh wave several small pulses appear which may be interpretated as longitudinal waves arriving at the transducer after reflection at the sides of the plate, and a slower transverse wave arriving shortly before the Rayleigh wave.

After some time, waves which are reflected from the boundaries of the plate appear. The shortest echo path has been calculated on the basis of the longitudinal wave velocity and the time of the earliest possible reflection is indicated in the figures, although it is not possible to clearly distinguish the echoes.

Transducer Type	8312	8313	8314
Voltage of transducer crystal (mV peak)	8,4	24	7,2
Vertical velocity of the surface wave (m/s peak)	7.10^{-5}	5.10^{-5}	9.10^{-5}

810031

Table 1. Peak signal voltages and corresponding peak vertical surface velocities of the surface waves

The absolute amplitude of the signal is measured in terms of voltage referred to the transducer crystal. Using the absolute surface wave calibration of the transducers this can be referred to the vertical velocity of the plate surface. Table 1 shows the peak values of the surface waves measured by the three transducers on the 50 mm plate at a distance of 100 mm from the point of excitation.

Pao et al. [11] have studied the wave generated by a step function force theoretically. Figs. 12 and 13 show the calculated surface response of a plate

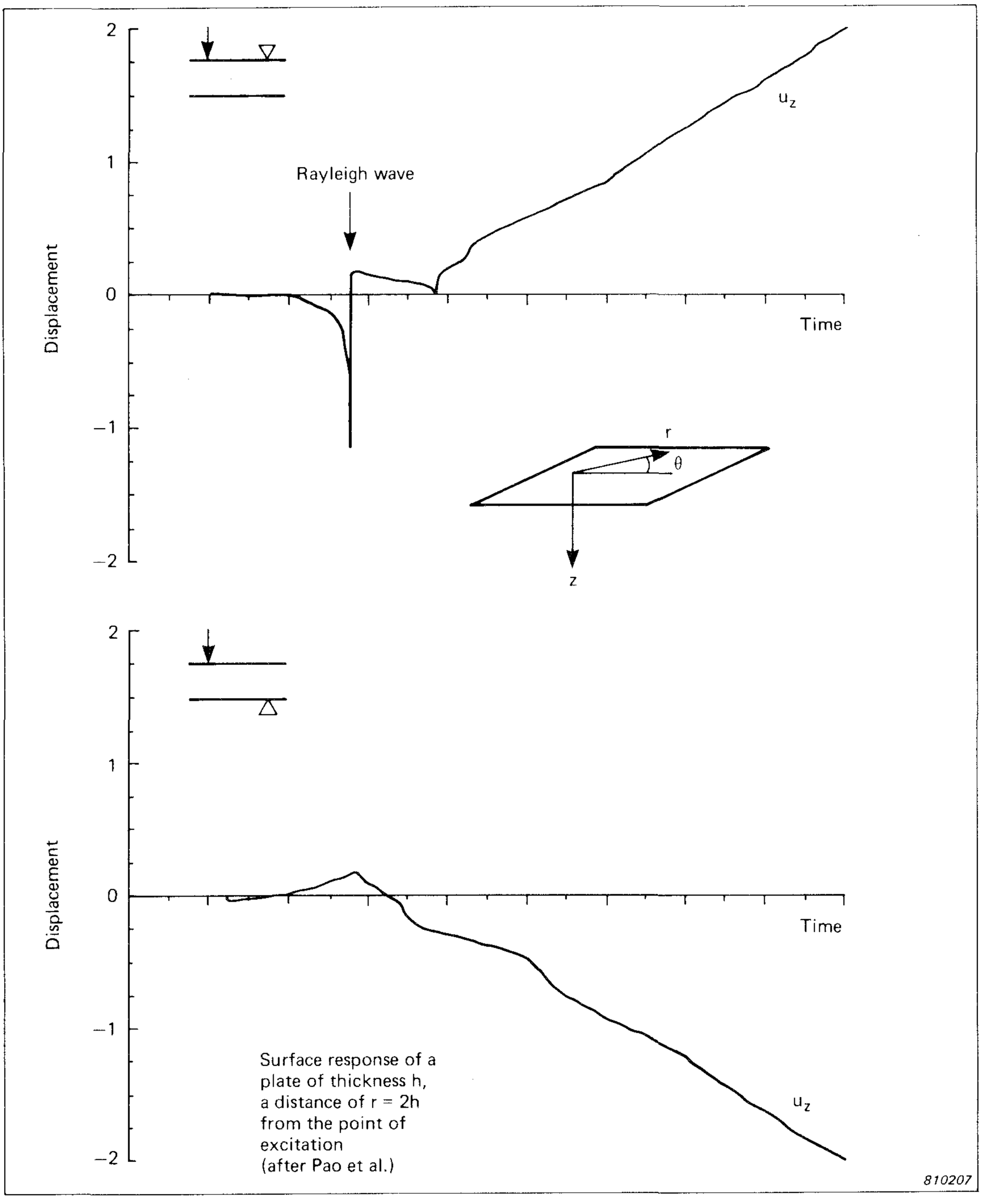

Fig. 12. Theoretical surface response of a plate of thickness h to a vertical surface force (r = 2h)

of thickness h to a vertical surface force; the near field response of both sides of the plate at a distance r = 2h (Fig. 12) and r = 4h (Fig. 13) from the point of excitation is shown. The vertical displacement, U_z, is plotted as a function of time, the upper surface of the plate being the plane z = 0 of the cylindrical coordinates (r, θ, z). The curves showing the response on the

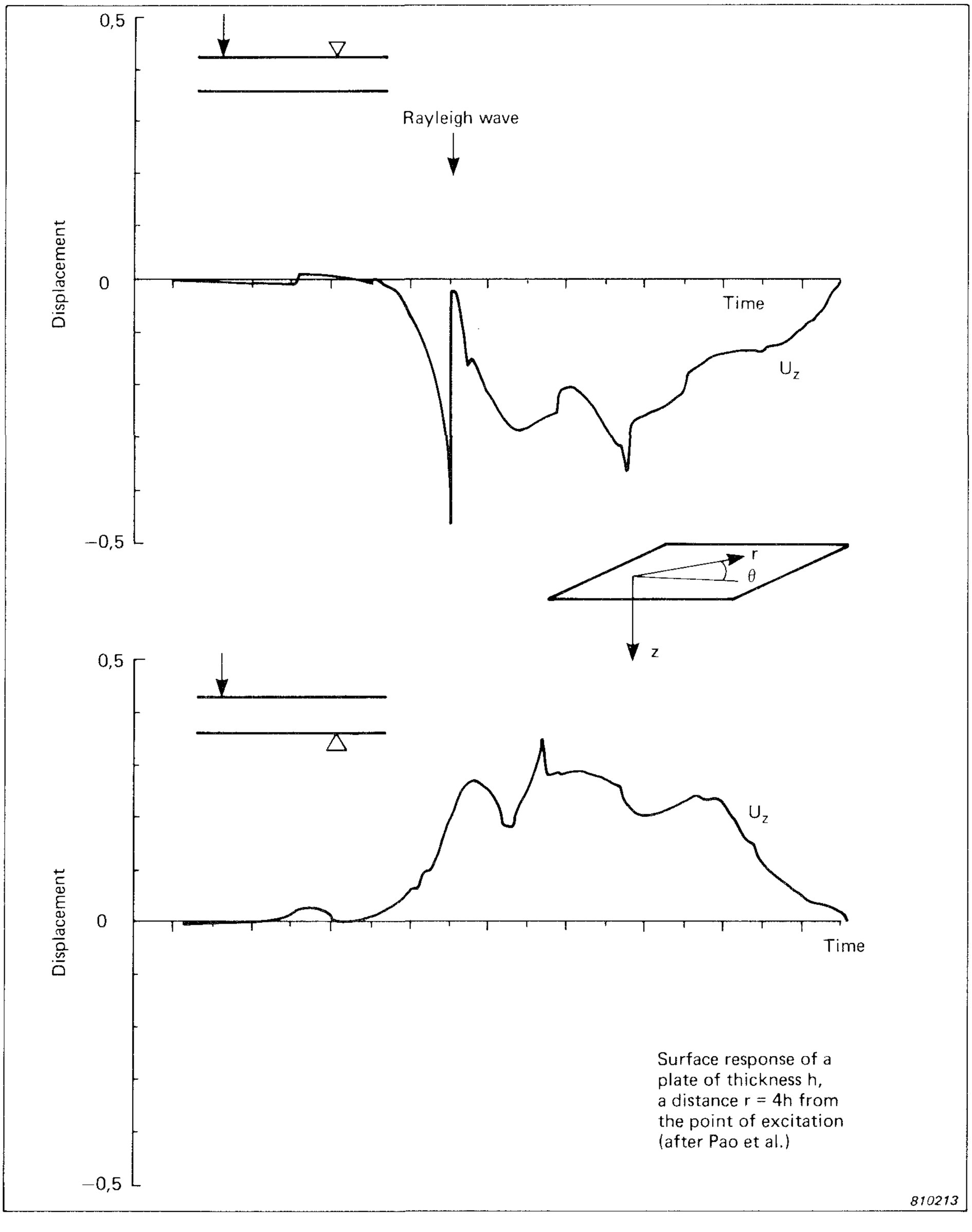

Fig. 13. Theoretical surface response of a plate of thickness h to a vertical surface force (r = 4h)

opposite side of the plate to the excitation force have been reflected about the time axis from Pao's original curves for comparison with the measured results given above (so that the vertical axes have the same direction relative to the transducer). The continued increase in displacement with time

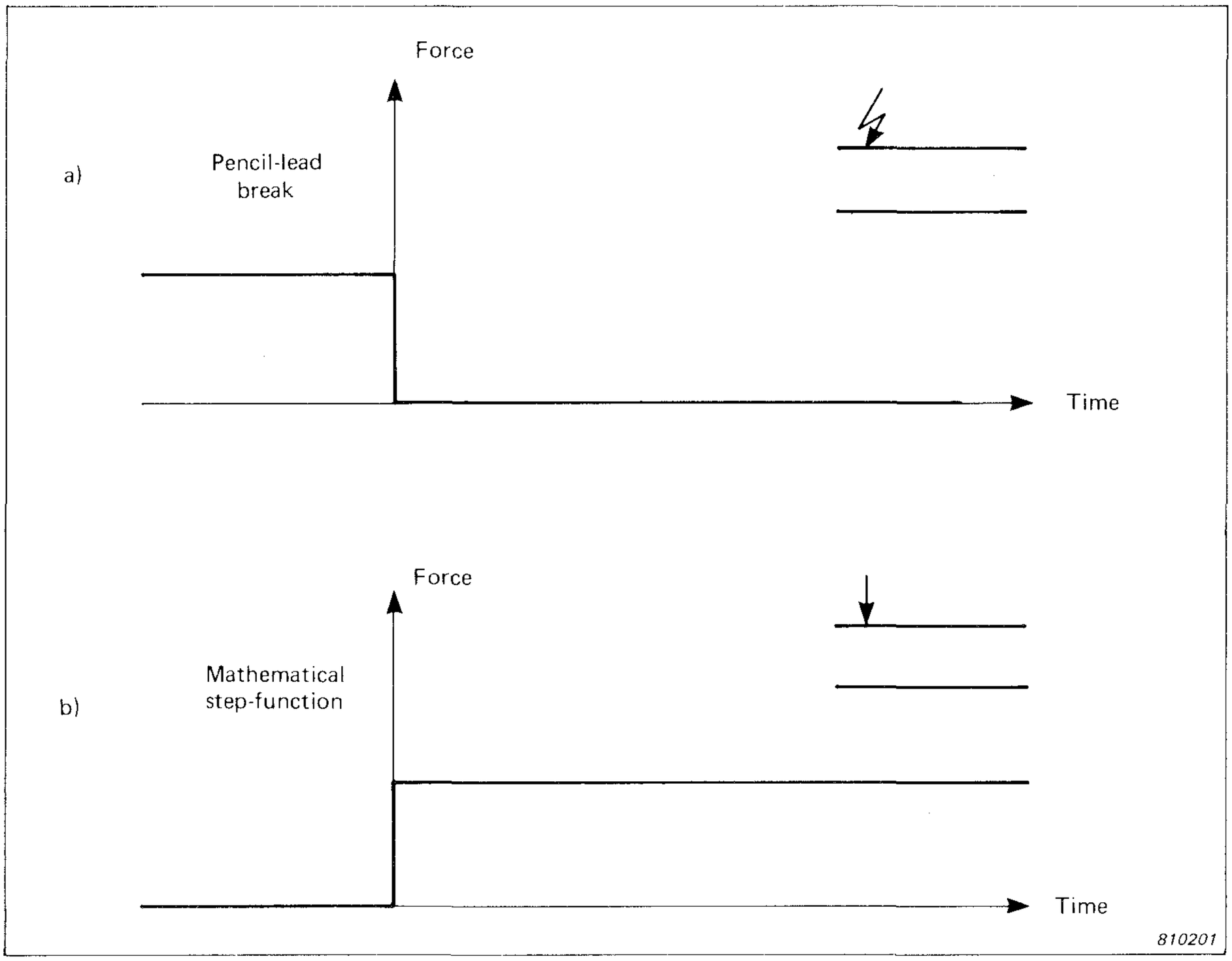

Fig. 14. a) Step function force produced by breaking a 0,5 mm pencil lead. b) Mathematical step function (Heaviside function) as used in Pao's calculation

shown in Figs. 12 and 13 is due to the theoretical step function force used by Pao (Fig. 14) which results in a continuous motion after the step occurs. For comparison of Fig. 9 with Figs. 12 and 13 it should be noted that the experimental results correspond to a velocity response while the theoretical curves show a displacement response. It can be seen that the experimental results verify the prediction of a small forerunning wave followed by a distinctive Rayleigh wave on the same side of the plate as the excitation force.

Results in the far field (Figs. 15 to 17) show approximately equal signal amplitudes on opposite sides of the plate. For lower frequency signals (i.e. those detected using transducer types 8312 and 8313) it can be seen that the leading wave ("front") appears with the same phase on either side of the plate. Later waves appear with opposite phase. This confirms the expectation that the leading waves are of the faster symmetric (longitudinal in plate centre line) type and the later waves are of the slower asymmetric (trans-

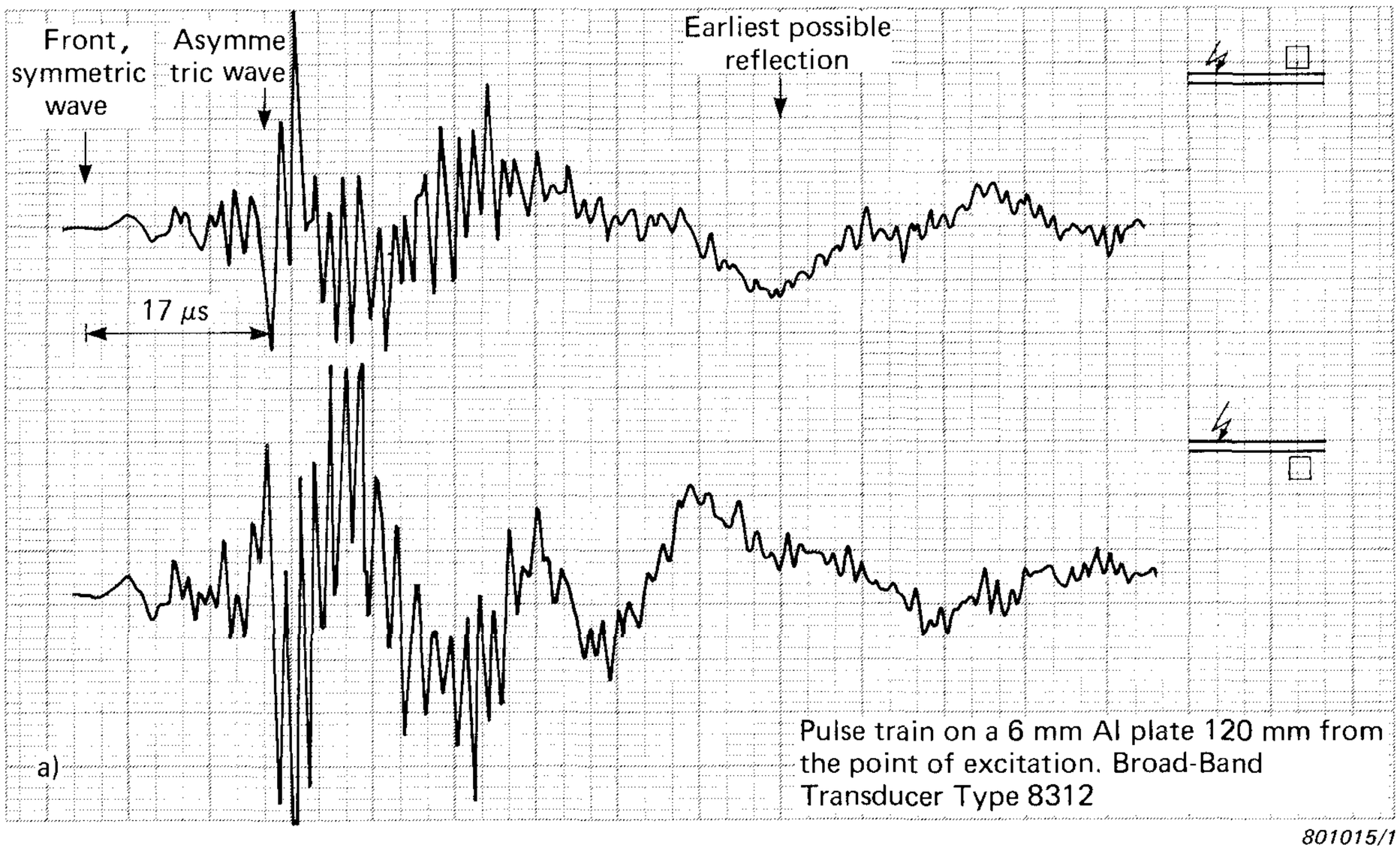

Fig. 15. Pulse trains recorded in the far acoustic field using Broad-Band Transducer Type 8312. Each figure shows the pulse train detected on opposite sides of the plate at a distance of
a) 120 mm from the point of excitation
b) 240 mm from the point of excitation

verse in centre line) type (Fig. 7). Calibration of the time scales is achieved using the source-to-transducer distance and the maximum zero-order symmetric (s_0) wave velocity to calculate the time elapsed since the pencil lead

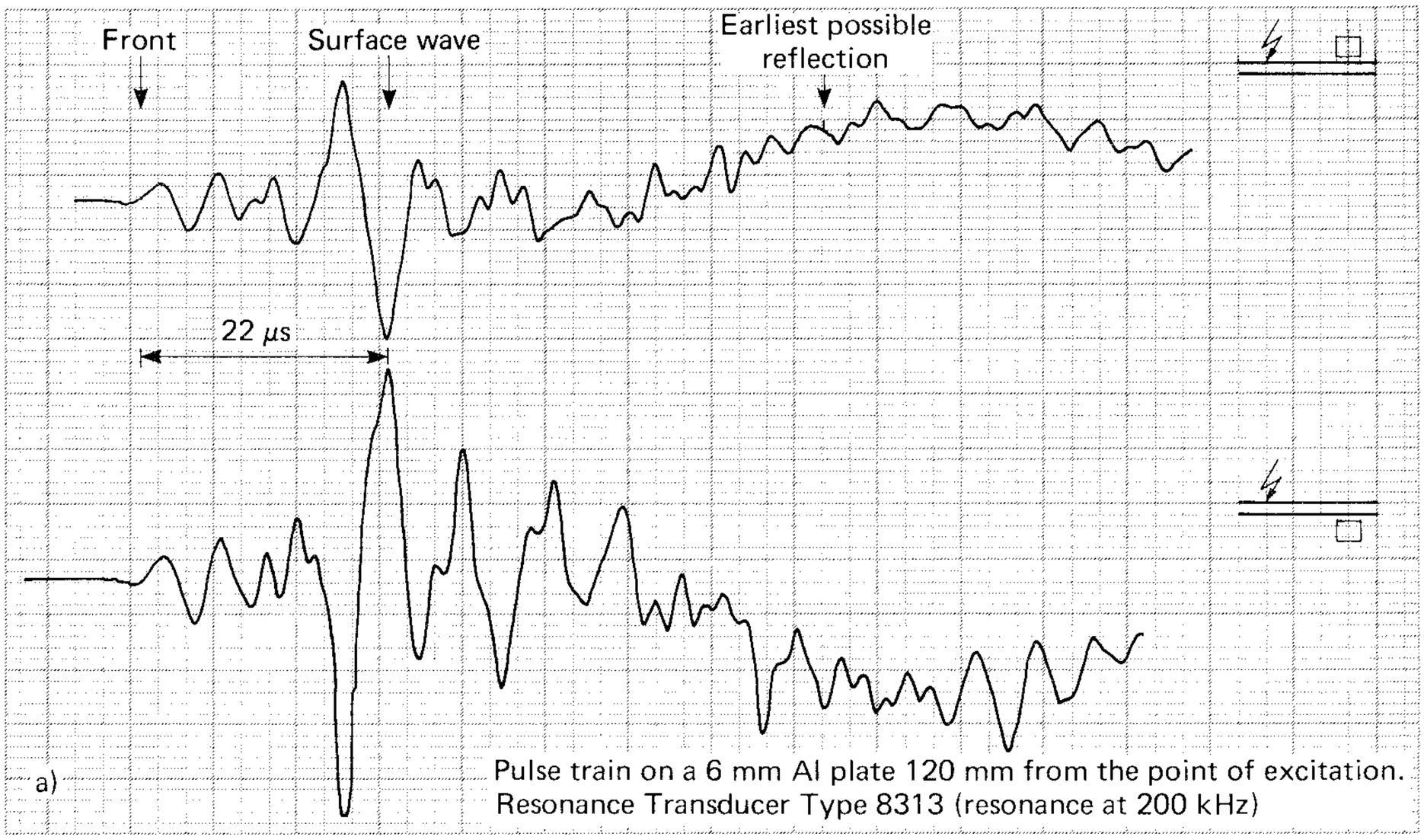

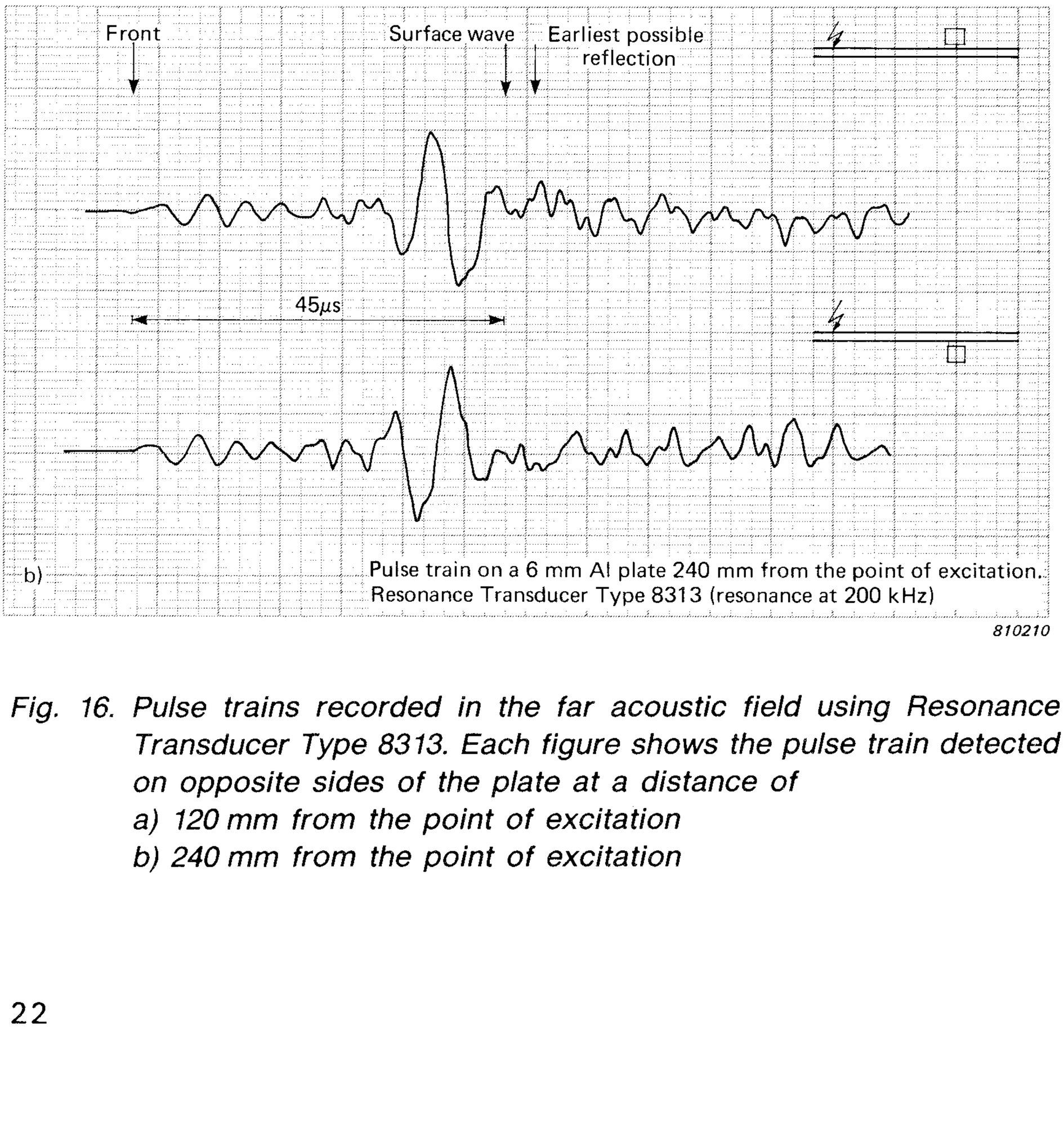

Fig. 16. Pulse trains recorded in the far acoustic field using Resonance Transducer Type 8313. Each figure shows the pulse train detected on opposite sides of the plate at a distance of
a) 120 mm from the point of excitation
b) 240 mm from the point of excitation

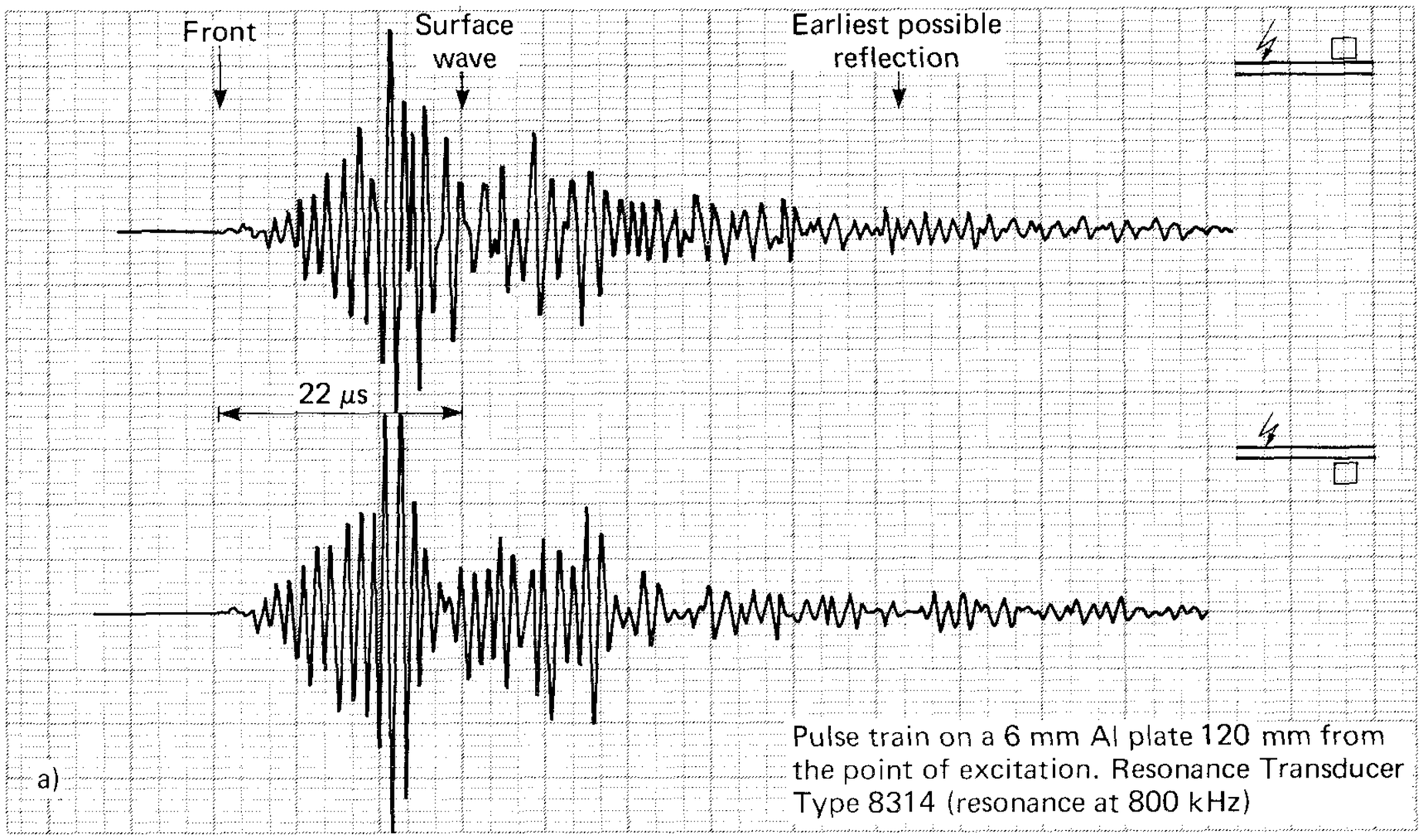

Fig. 17. Pulse trains recorded in the far acoustic field using Resonance Transducer Type 8314. Each figure shows the pulse train detected on opposite sides of the plate at a distance of
a) 120 mm from the point of excitation
b) 240 mm from the point of excitation

was broken. Using the surface wave velocity, the expected arrival time of a Rayleigh wave can then be found. The resulting time differences between the arrival of the symmetric wave and the expected Rayleigh wave are shown in the figures. In fact, it is not possible to identify a Rayleigh wave in this case. For transducer Type 8313 two distinct wavefronts can be identified whereas the results using Type 8314 show a less distinct front. Referring to the plate wave mode diagram (Fig. 7), it can be seen that two wave modes exist for a 6 mm plate at 200 kHz (thickness —frequency product = 1,2 mmMHz) and five modes are present at 800 kHz (thickness — frequency product = 4,8 mmMHz). It should be noted that although the plate wave mode diagram shown in Fig. 7 is valid for steel, the values are only slightly different for aluminium.

The arrival time differences can be established by correlation techniques, first threshold passage or using the peak level of the pulse. However reflections can cause complexities in correlation and peak measurements. None of the methods is ideal when one considers such factors as varying frequency bandwidth of the detector and varying type, size and position of events. It will also be apparent that calibration with an artificial source may be misleading and a random source, capable of producing various types of event, should be used, preferably on both sides of the plate. From experiments and extensive studies of real AE data, it has been found that good results can be obtained using software that considers two velocities corresponding to the two fundamental wave modes.

2. Secondary Problems:
Apart from the problem of determining the wave modes present, difficulties arise due to phase uncertainty and superposition of multiple events.

Since the phase of the source is not known there will always be some uncertainty, even under otherwise ideal conditions. With a 200 kHz transducer this is of the order of 3 μs or 10 to 15 mm.

Electromagnetic interference should be minimized by the use of proper instrumentation although it may not be possible to completely eliminate it. Since such signals tend to trigger several channels simultaneously, the transducers should be arranged in arrays which cannot be simultaneously triggered by real AE events. The rectangular array shown in Fig. 18a) has multiple symmetry; an event occurring at the mid-point of the array will trigger all four channels simultaneously. By moving one of the transducers (Fig. 18b) the multiple symmetry is avoided and an AE event cannot possibly trigger all the channels at the same time. The software can then easily recognize and reject most types of signals caused by electromagnetic interference.

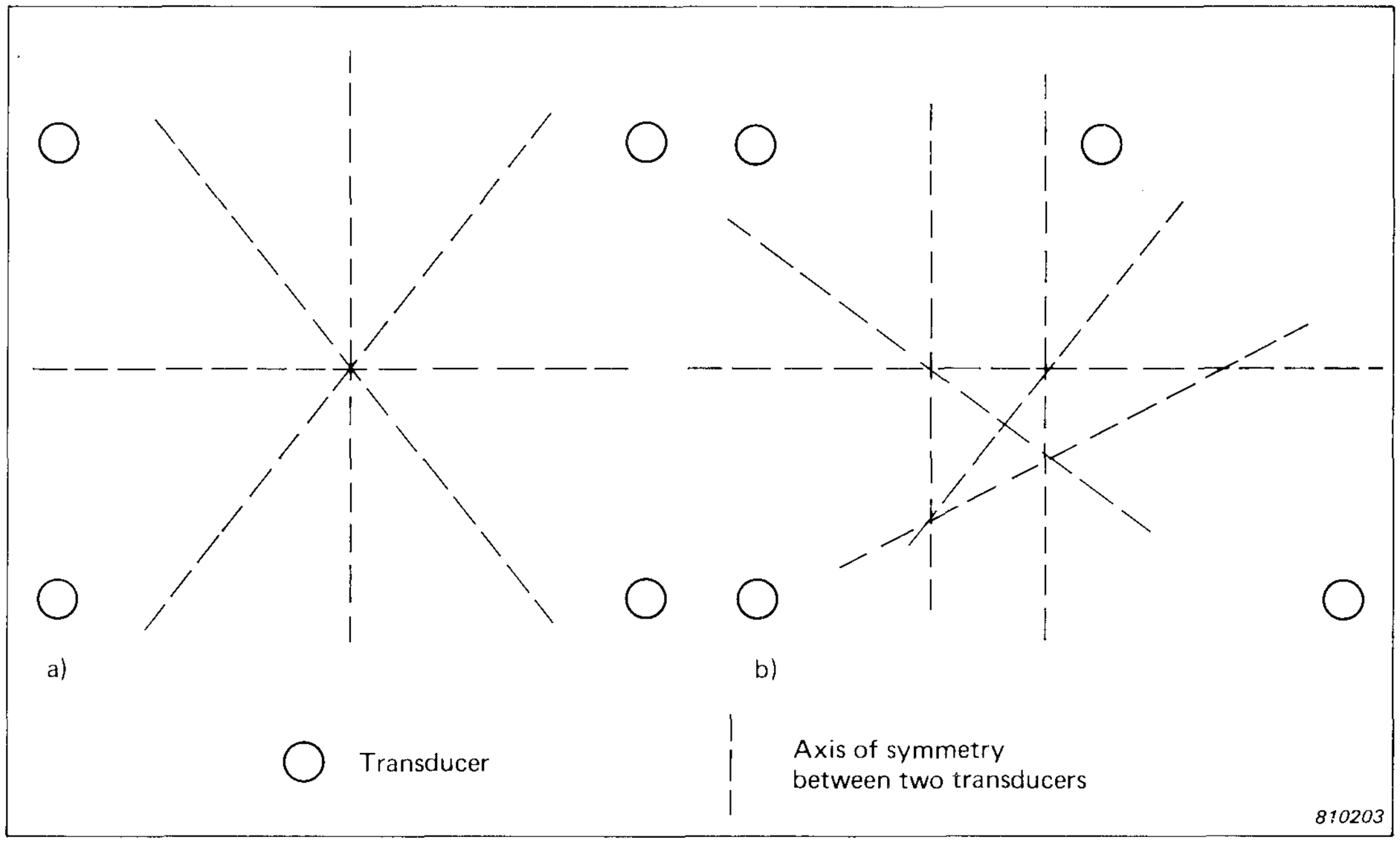

Fig. 18. Symmetry of transducer arrays. a) The rectangular array has multiple symmetry and an event at the centre will trigger all channels simultaneously b) This can be avoided by moving one of the transducers

In practice, the signals triggering the different channels may not originate from the same event. Such false data may yield no location at all or a location which, almost certainly, will be incorrect. The probability of this type of data occurring depends on the ratio between the event rate and the travel time from one AE source to another, or to a transducer. If the event rate is very high the distance between the transducers should be reduced or the threshold of detection (i.e. the trigger level) should be raised to reduce the event rate. Although the problem cannot be completely avoided, it is not very significant in practice.

Accuracy Of The Resulting Location

Errors in the measurement of the relative arrival times will affect the source location calculations in a complex manner. This may be shown mathematically by considering a pair of transducers situated at the polar coordinates (0,5; 90°) and (0,5; 270°) as shown in Fig. 19. The spacing of the transducers is taken to be unity. From the measured time delay, Δt, the path difference (δ) can be calculated:

$$\delta = \Delta t \cdot v \qquad (1)$$

where v = the wave velocity.

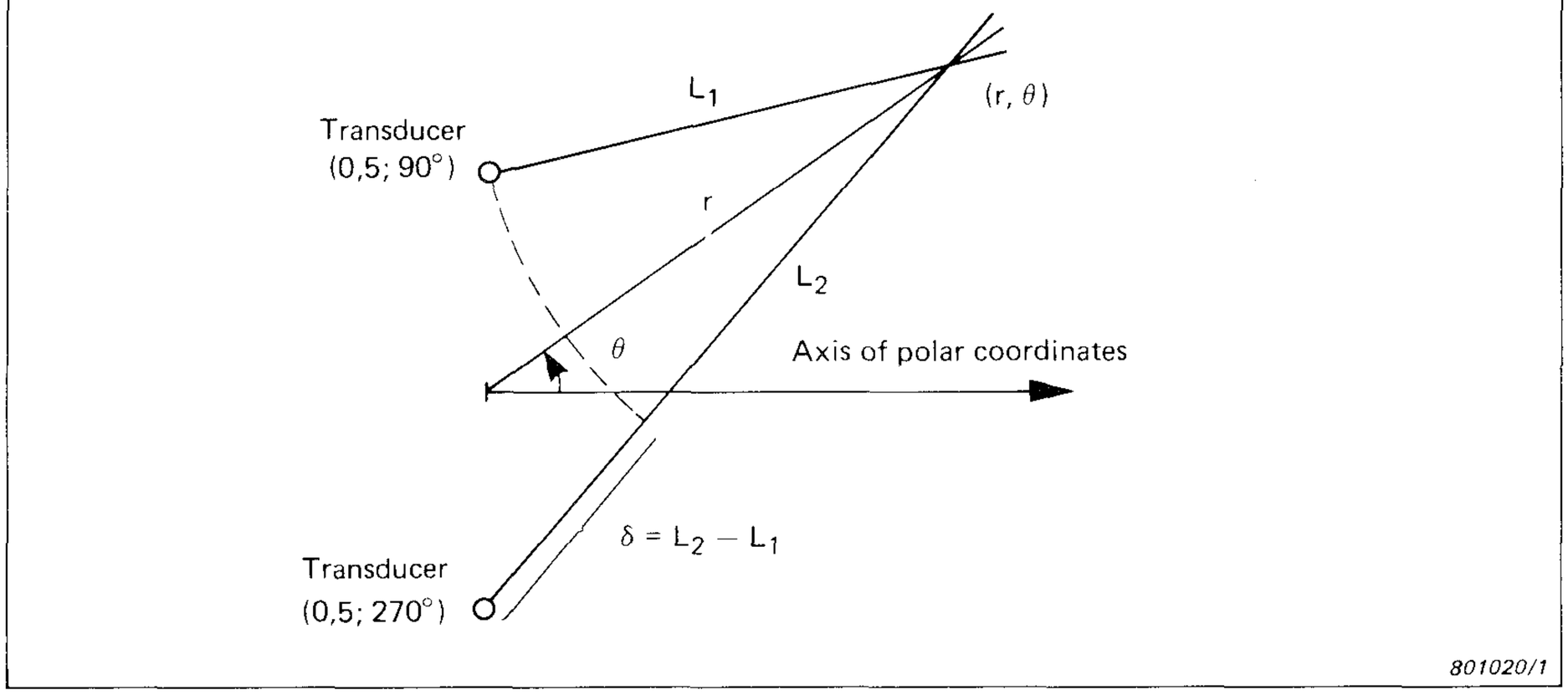

Fig. 19. Pair of transducers with unity spacing located at the polar coordinates (0,5; 90°) and (0,5; 270°)

The polar coordinates of the source (r; Θ) must satisfy the equation of a hyperbola:

$$r = \frac{\delta}{2}\sqrt{\frac{1-\delta^2}{\sin^2\theta - \delta^2}} \qquad (2)$$

or the equivalent:

$$\sin\theta = \frac{\delta}{2r}\sqrt{1-\delta^2+4r^2} \qquad (3)$$

Both equations define a hyperbola with the transducers at the focii.

Differentiating these equations with respect to δ we obtain:

$$\frac{dr}{d\delta} = \frac{\delta^4 + (1-2\delta^2)\sin^2\theta}{2\sqrt{(\sin^2\theta - \delta^2)^3\,(1-\delta^2)}} \qquad (4)$$

and

$$\frac{d\theta}{d\delta} = \frac{1-2\delta^2+4r^2}{\sqrt{(1-\delta^2+4r^2)\,(4r^2-\delta^2)\,(1-\delta^2)}} \qquad (5)$$

respectively.

Using equations 4 and 5 the accuracy in determining the position of the source using this pair of tranducers can be plotted in terms of r and Θ.

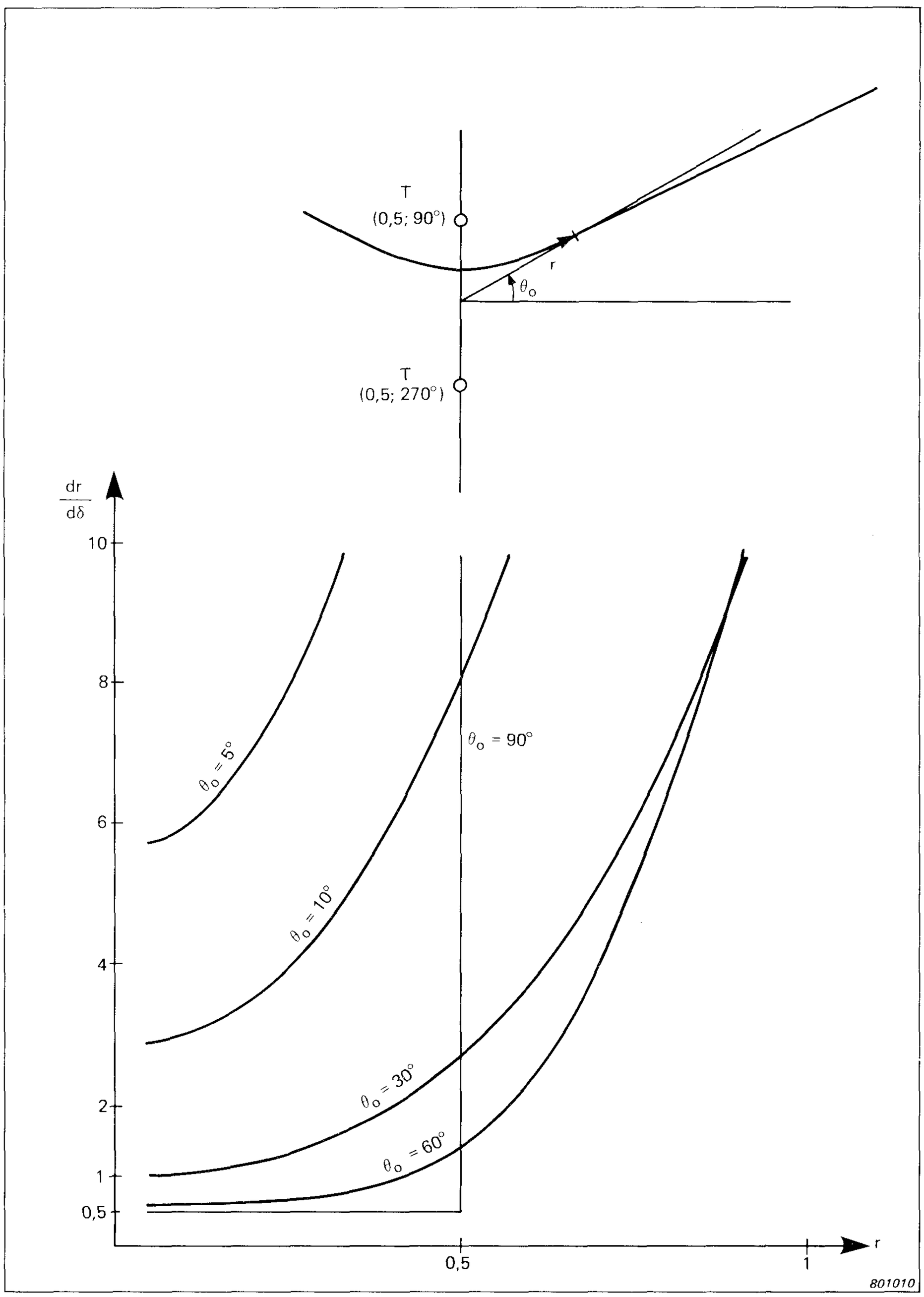

Fig. 20. Accuracy of distance (r) for a known direction (θ). $dr/d\delta$ is plotted as a function of r for various values of the parameter θ

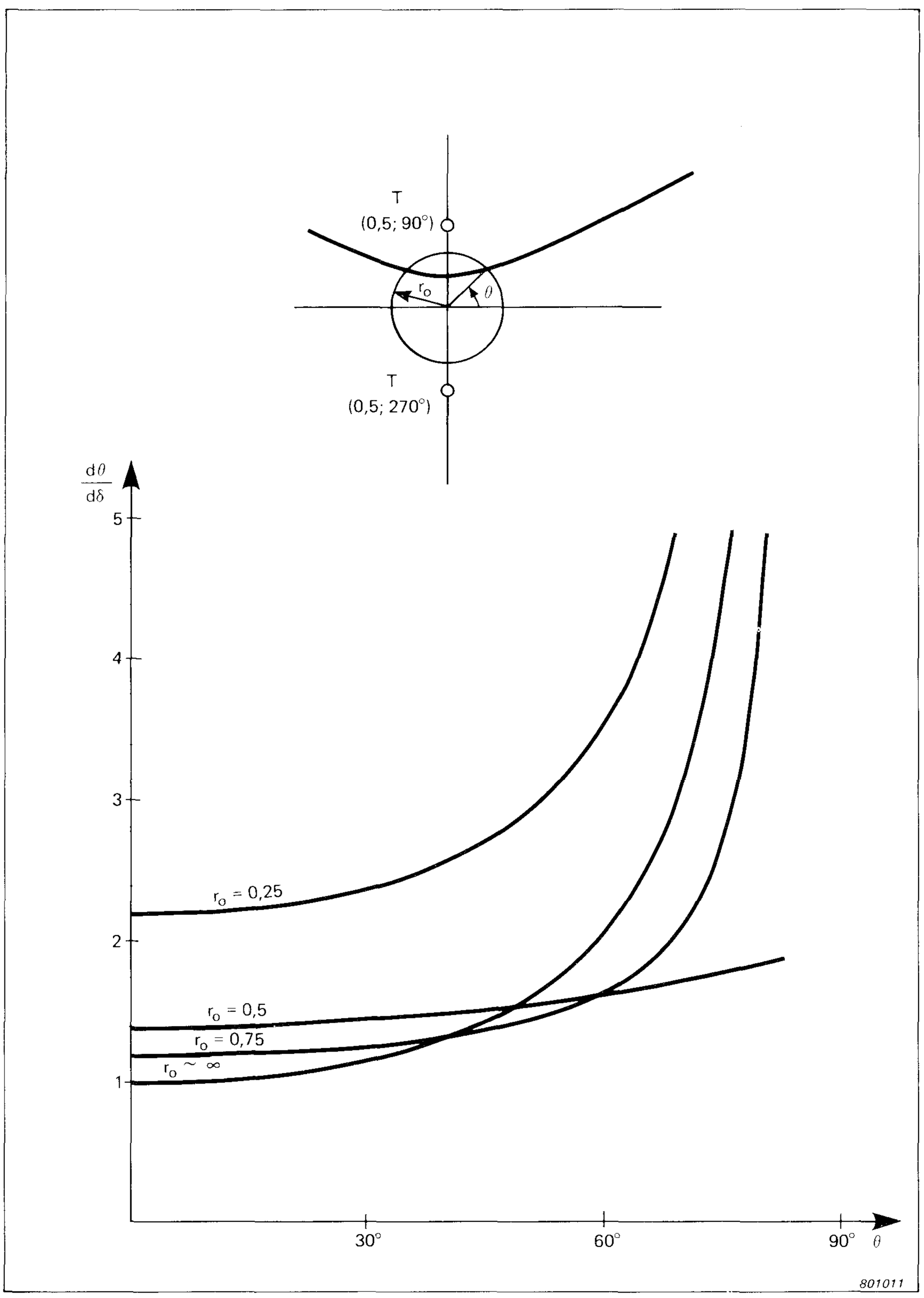

Fig. 21. Accuracy of direction (θ) for a known distance (r). $d\theta/d\delta$ is plotted as a function of θ for various values of the parameter r

Fig. 20 shows curves of $dr/d\delta$ against r for some values of Θ, i.e. assuming the direction (Θ) is known, the curves show how accurately the distance (r) to the source can be determined. It can be seen that apart from angles near 0°, the accuracy is good within a radius extending to the transducers. Outside this range the error increases rapidly. It is evident that the accuracy is greatest near the midpoint between the two transducers. The curves illustrate the case for a constant accuracy in Δt and correct assumption of the wave velocity. $dr/d\delta$ should be multiplied by r to account for a situation in which an error is introduced in the wave velocity since δ is proportional to r.

Fig. 21 shows curves of $d\Theta/d\delta$ against Θ for some values of r, i.e. assuming the distance (r) is known, the curves show how accurately the direction (Θ) of the source can be determined using these transducers. The directional accuracy is good except near the axis through the transducers and, in general, does not depend significantly on the distance from the origin except at a distance of r = 0,5 resulting in singularity at the transducers.

Both figures confirm that there are large variations in the spatial resolution. In practice this means that source location algorithms based on iterative methods or tables may run into problems (numeric instability). It can also be concluded that a pair of transducers cannot accurately locate a source which is near to or "behind" either transducer since the uncertainty tends to infinity in this region.

The resolution pattern obtained using a set of three transducers is perhaps best visualized in Fig. 2. In this figure hyperbolae are drawn for constant intervals of δ. The form and shape of the area between the intersecting hyperbolae illustrate the pattern of resolution. In conclusion it may be said that high location accuracy can only be expected inside the region spanned by the transducer array.

Some Guidelines for Measurement Procedure

In practice, AE source location procedure reduces to measuring the relative arrival times of the AE signal and calculating the path differences defined in equation 1 and the intersection of the associated hyperbolae.

Relative arrival times, referred to one of the transducers, can be measured using an analyzer such as the B & K Acoustic Emission Pulse Analyzer Type 4429 (Fig. 22). The arrival times may be recorded for later analysis or fed directly via a digital interface bus for on-line processing using a calculator. Programming normally allows for the transducer coordinates and wave

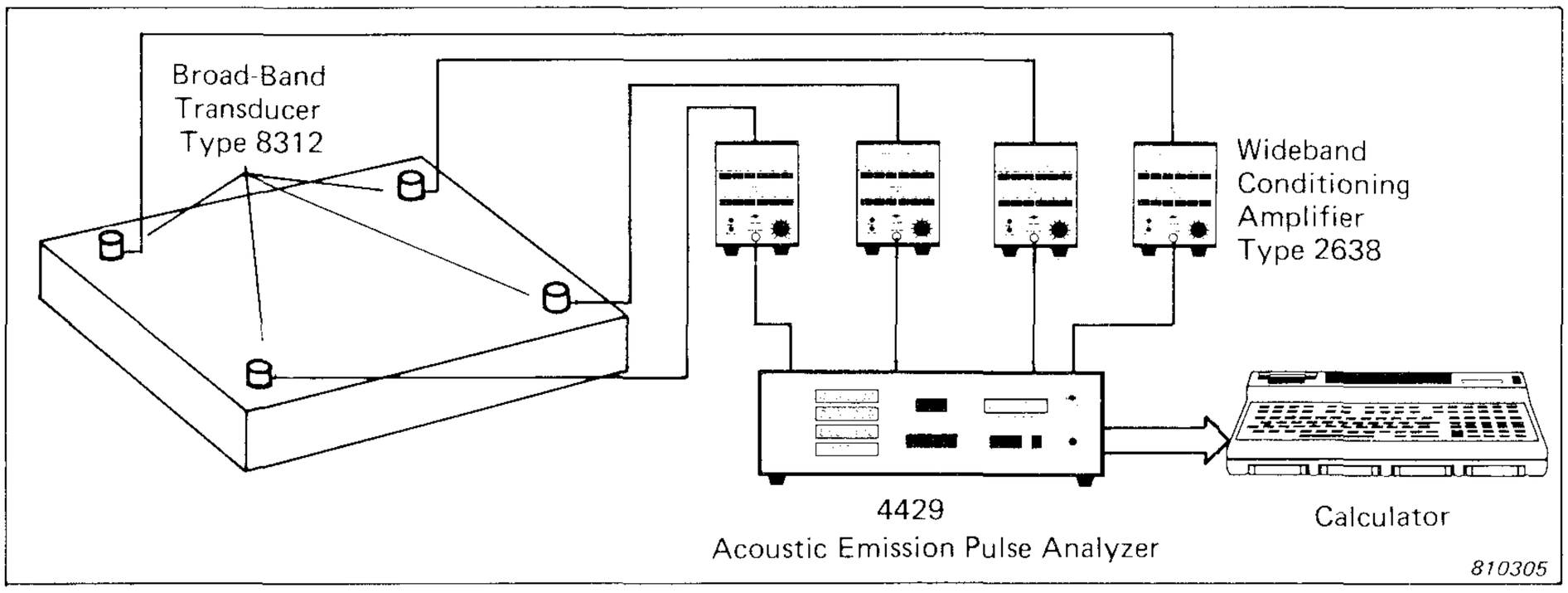

Fig. 22. Measurement of AE source location

velocity value to be written in after calibration procedures on the structure are made. Sophisticated programs exist which consider two wave velocities.

Optimum performance from an AE source location system is achieved by minimizing the errors which may occur in determining the wave velocity and the measured arrival times used in the algorithm. By dividing the structure into homogeneous sections and segmenting transducer arrays accordingly, the wave velocity can be assumed to be uniform within that area. Areas which are of particular interest should be covered by the mid-region of the array where the spatial resolution is best and ambiguous solutions are avoided. The wave attenuation and velocity should be checked in each section and wave mode diagrams referred to, according to the structure dimensions and frequency range of detection. Different types of calibration sources should be used, preferably at various positions on the surface, and the channel triggering adjusted. Event rates which are excessive relative to the transducer spacing should be avoided by raising the trigger level (or decreasing the size of the array) and electromagnetic interference should be minimized. The extent to which these guidelines will prove effective is necessarily dependent on the individual conditions of the experiment and some compromise is unavoidable.

Conclusion

An examination of the uncertainties that, in theory, may occur even in relatively simple structures illustrates the difficulty in applying AE source location methods and perhaps explains the mixed success of the technique. Experience shows, however, that although some incorrect data is unavoidable, it is possible to obtain good results by applying statistical methods to the measured data.

References

[1] LICHT, T. R. — Acoustic Emission. Bruel & Kjær Technical Review, No. 2 — 1979.

[2] ONOE, M. — Japanese experience in laboratory and practical application of acoustic emission to welded structures. Institute of Industrial Science. University of Tokyo, Roppongi, Tokyo, Japan.

[3] HARDY, H. R., Jr. — "Evaluating the Stability of Geologic Structures Using Acoustic Emission". Monitoring Structural Integrity by Acoustic Emission, ASTM STP 571. American Society for Testing and Materials, 1975, pp. 80-106.

[4] PARRY, D. L. — "Industrial Application of Acoustic Emission Analysis Technology," Ibid, pp. 150-183.

[5] BLAKE, W., LEIGHTON, F. & DUVALL, W. I. — Microseismic Techniques for Monitoring the Behaviour of Rock Structures. U.S. Bureau of Mines, Bulletin 665.

[6] TOBIAS, A. — Acoustic Emission Source Location in Two Dimensions by an Array of Three Transducers. Non-Destructive Testing, February 1976, pp. 9-12

[7] ASTY, M. — Acoustic Emission Source Location on a Spherical or Plane Surface. NDT International, October 1978, pp. 223-226.

[8] OBATA, Y. & BENTLEY, P. G. — Acoustic Emission Test on a 1 Metre Diameter Pressure Vessel with a 60% Artificial Defect. 4 th International Meeting on Acoustic Emission, Tokyo, 18 Sept. 1978.

[9] KAYE, G. W. C. & LABY, T. H. — Tables of physical and chemical constants. 13 th ed. 1966. Longmans, Green & Co. Ltd.

[10] VIKTOROV, I. A. "Rayleigh and Lamb Waves". Plenum Press, New York, 1967

[11] PAO, Y-H., GAJEWSKI, R. R. & CERANOGLU, A. N. Acoustic Emission and Transient Waves in an Elastic Plate. J. Acoust. Soc. Am., Vol. 65, No. 1, January 1979, pp. 96-105.

APPENDIX A

Algorithm for Source Location [6]

The algorithm given below provides a method for direct solution of the point of intersection of two hyperbolae. Appendix B contains a program listing for a HP-41C calculator based on this algorithm for a particular transducer array. The algorithm itself, however, is not resricted by the array geometry.

Three transducers are arranged in an array at the cartesian coordinates (0, 0), (x_1, y_1) and (x_2, y_2). The hyperbolae are defined by the measured relative arrival times 0, t_1 and t_2 at the respective transducers and the wave velocity v. The source location (x, y) is given as follows:

$$(x_1^2 + y_1^2) - (v^2 \cdot t_1^2) \Rightarrow A_1 \qquad (I)$$

$$(x_2^2 + y_2^2) - (v^2 \cdot t_2^2) \Rightarrow A_2 \qquad (II)$$

$$\text{If} \quad A_1x_2 - A_2x_1 \geqslant 0 \text{ , then } \tan^{-1}\frac{A_1y_2 - A_2y_1}{A_1x_2 - A_2x_1} \Rightarrow B \qquad (III)$$

$$\text{If} \quad A_1x_2 - A_2x_1 < 0 \text{ , then } \tan^{-1}\frac{A_1y_2 - A_2y_1}{A_1x_2 - A_2x_1} + \pi \Rightarrow B \qquad (IV)$$

$$\cos^{-1}\frac{A_2 \cdot v \cdot t_1 - A_1 \cdot v \cdot t_2}{\sqrt{(A_1x_2 - A_2x_1)^2 + (A_1y_2 - A_2y_1)^2}} \Rightarrow C \qquad (V)$$

which give two solutions $(r_1; \theta_1)$ and $(r_2; \theta_2)$ for the source location in polar coordinates $(r; \theta)$:

$$r_1 = \frac{A_1}{2(x_1 \cos\theta_1 + y_1 \sin\theta_1 + v \cdot t_1)} \quad \text{where } \theta_1 = B - C \qquad (VI)$$

and

$$r_2 = \frac{A_1}{2(x_1 \cos\theta_2 + y_1 \sin\theta_2 + v \cdot t_2)} \quad \text{where } \theta_2 = B + C \qquad (VII)$$

If either r_1 or r_2 is negative, then that solution is invalid.

The corresponding solutions in cartesian coordinates are given by:

$$(x,y)_1 = (r_1 \cos\theta_1 , r_1 \sin\theta_1) \qquad \text{(VIII)}$$

and

$$(x,y)_2 = (r_2 \cos\theta_2 , r_2 \sin\theta_2) \qquad \text{(IX)}$$

The double solution only occurs in the areas close to and "behind" the transducers. To resolve the ambiguity, a fourth transducer at the point (x_3, y_3) with measured relative arrival time t_3 is used and the correct source location is found as follows:

$$\frac{\sqrt{(x-x_3)^2+(y-y_3)^2} - \sqrt{x^2+y^2} - v \cdot t_3}{\sqrt{(x-x_3)^2+(y-y_3)^2}} \Rightarrow \dot{D} \qquad \text{(X)}$$

D should be calculated for both solutions of (x, y) found above and the coordinate pair resulting in the smallest numerical value of D should be preferred.

APPENDIX B

Program For Source Location

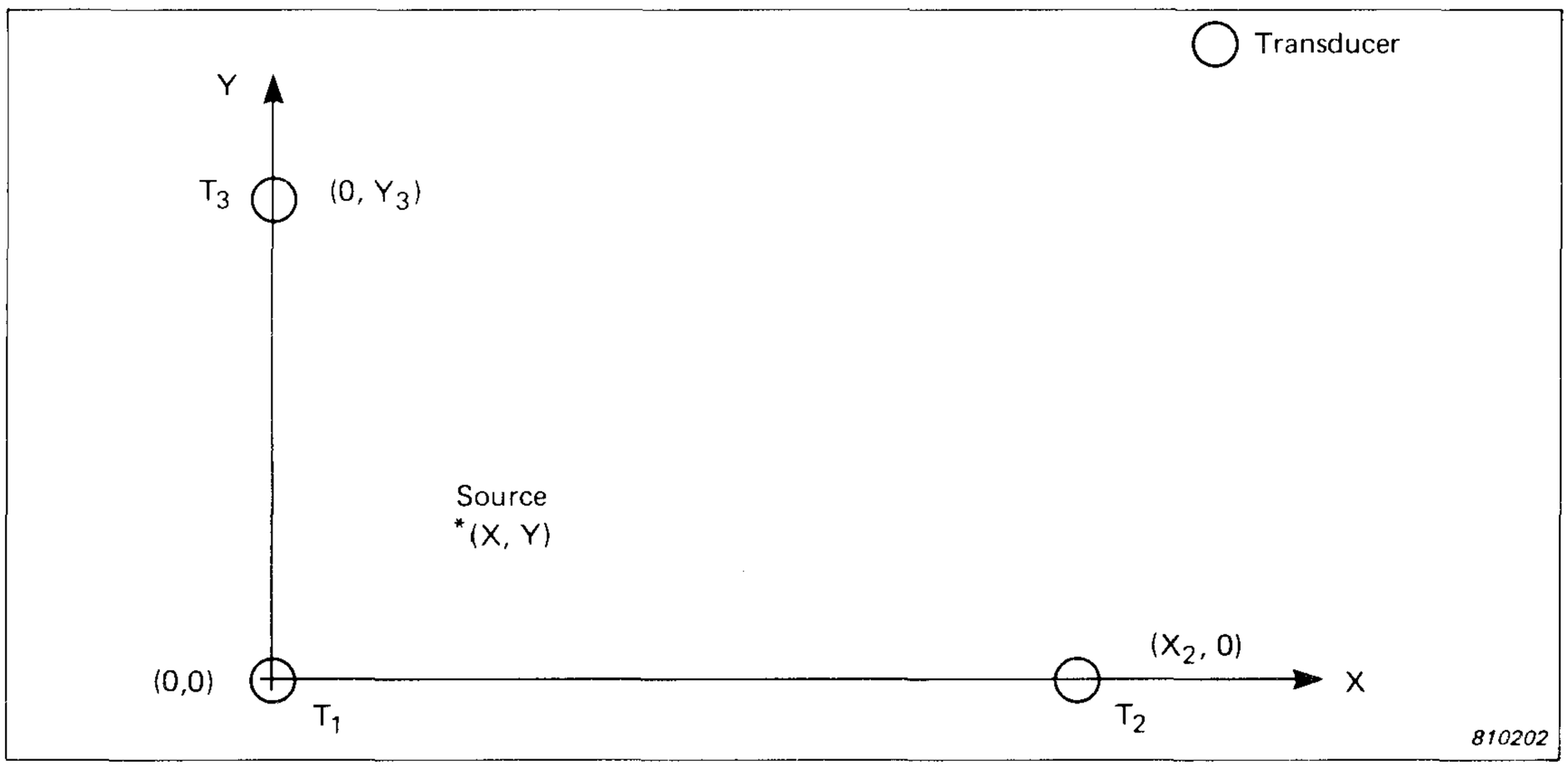

Fig. B1. Right-angled triangular array of transducers

A program listing for an HP-41C Alphanumeric Programmable Scientific Calculator is given below. * The program calculates the source position in rectangular coordinates (X, Y) for the right-angled triangular array of three transducers shown in Fig. B1 when the arrival times at the three transducers (T1, T2, & T3) are given in micro-seconds. The program yields values in the 1'st quadrant (i.e. only positive values of X and Y). Standard data already written into the program is as follows:

X2 = 50 (length unit)
Y3 = 40 (length unit)
V = 0,3 where V is the wave velocity in (length unit)/micro-second.

The standard data is optional and other values of X2, Y3 and V may be chosen whilst running the program. The procedure for running the program once it is loaded is as follows:

1. Turn the calculator on.
2. Assign the program name "LOCAL" to X ⇌ Y by keying the following instruction: ASN ALPHA "LOCAL" ALPHA X ⇌ Y.
3. Assign the program name "NEW" to SIN by keying the following instruction: ASN ALPHA "NEW" ALPHA SIN.
4. Assign the program name "NCAL" to R↓ by keying the following instruction: ASN ALPHA "NCAL" ALPHA R↓.
5. Put the calculator into the USER mode.
6. Press X ⇌ Y. The calculator display will briefly show "NEW DATA > SIN" to indicate that new data can be inserted in place of the standard data for X2, Y3, and V by pressing SIN. (If new standard data is chosen by pressing SIN, go to step 6a). If this is not done the standard data given above for these parameters is loaded and the calculator asks for the measured arrival time at transducer 1 by displaying "T1 ?".
7. Insert the arrival time for transducer 1 (e.g. 0) and press R/S.
8. The calculator asks for arrival time 2 by displaying "T2 ?". Insert the value for T2 (e.g. 80) and press R/S.
9. Calculator displays "T3 ?". Insert the arrival time T3 (e.g. 60) and press R/S. After approximately 10 seconds calculation the source location is displayed (e.g. "X, Y = 12, 10"). If a printer is used the coordinates will also be printed. If the input data does not yield a valid solution, the display shows "INVALID". This is also printed.
10. To repeat the calculation for new values of arrival time using the same standard data for X2, Y3 and V, press X ⇌ Y. If new standard data is required, press R↓ (this turns the calculator off in a neutral mode), turn the calculator on again and proceed from step 5.

* A similar program is available for a Texas TI-59 instrument.

```
01◆LBL "LOCAL"
02 FS? 00
03 GTO 03
04 GTO a
05◆LBL 03
06 "T1 ?"
07 PROMPT
08 ENTER↑
09 STO 21
10 "T2 ?"
11 PROMPT
12 -
13 CHS
14 RCL 17
15 *
16 STO 11
17 X↑2
18 CHS
19 RCL 15
20 +
21 XEQ b
22 STO 02
23 "T3 ?"
24 PROMPT
25 RCL 21
26 -
27 RCL 17
28 *
29 STO 12
30 X↑2
31 CHS
32 RCL 16
33 +
34 XEQ b
35 STO 03
36 RCL 18
37 *
38 STO 00
39 RCL 03
40 ENTER↑
41 RCL 11
42 *
43 RCL 02
44 ENTER↑
45 RCL 12
46 *
47 -
48 RCL 02
49 ENTER↑
50 RCL 19
51 *
52 CHS
53 RCL 00
54 R-P
55 X<>Y
56 PI
57 +
58 STO 07
59 RDN
60 /
61 1
62 +
63 XEQ b
64 2
65 -
66 CHS
67 XEQ b
68 CHS
69 1
70 +
71 ACOS
72 CHS
73 RCL 07
74 +
75 STO 10
76 COS
77 RCL 18
79 *
79 RCL 11
80 +
81 2
82 *
83 RCL 02
84 /
85 X=0?
86 XEQ b
87 1/X
88 X<0?
89 GTO 01
90 RCL 10
91 X<>Y
92 P-R
93 STO 04
94 X<>Y
```

810029

Fig. B2. AE source location program listing for HP-41 C pocket calculator

```
 95 STO 05
 96 X<>Y
 97 X<0?
 98 GTO 01
 99 .5
100 +
101 INT
102 RCL 05
103 X<0?
104 GTO 01
105 ENTER↑
106 .5
107 +
108 100
109 /
110 +
111 "PRX"
112 "ADV"
113 "X,Y="
114 ARCL X
115 AVIEW
116 STOP
117◆LBL 01
118 "INVALID"
119 PRA
120 PROMPT
121◆LBL b
122 X>0?
123 GTO 02
124 1
125 +
126 X<0?
127 GTO 01
128 RCL 09
129◆LBL 02
130 RTN
131◆LBL a
132 SF 00
133 RAD
134 FIX 2
135 50
136 STO 18
137 40
138 STO 19
139 .3
140 STO 17
141 .1
142 STO 09
143 RCL 18
144 X↑2
145 STO 15
146 RCL 19
147 X↑2
148 STO 16
149 RCL 19
150 ENTER↑
151 RCL 18
152 /
153 CHS
154 STO 14
155 "NEW DAT A>SIN"
156 AVIEW
157 PSE
158 GTO "LOCAL"
159◆LBL "NCAL"
160 CF 00
161 DEG
162 OFF
163◆LBL "NEW"
164 "X1,Y1=0,0"
165 AVIEW
166 PSE
167 "X2,Y2=?,0"
168 PROMPT
169 STO 18
170 "X3,Y3=0,?"
171 PROMPT
172 STO 19
173 "V=?"
174 PROMPT
175 STO 17
176 RCL 18
177 X↑2
178 STO 15
179 RCL 19
180 X↑2
181 STO 16
182 RCL 19
183 ENTER↑
184 RCL 18
185 /
186 CHS
187 STO 14
188 GTO "LOCAL"
189 .END.
```

810030

6. a) If new standard data for X2, Y3 and V is required, i.e. after pressing SIN in step 6, proceed as follows:
   b) The display shows briefly "X1, Y1 = 0,0" to indicate that transducer 1 must remain at the point (0, 0). The display then shows "X2, Y2 = ?, 0". Insert the new value for X2 and press R/S.
   c) Display shows "X3, Y3 = 0, ?". Insert the new value for Y3 and press R/S.
   d) Display shows "V = ?". Insert the new value for V and the display shows "T1 ?". Continue as from step 7 above.

To turn the calculator off in a neutral mode, press R↓.

APPENDIX C

In-Situ Sensitivity Calibration of Acoustic Emission Systems
The European Working Group on Acoustic Emission agreed to the following at its meeting in Senlis, France, Oct. 9'th 1980:

*It will be a great help if reports of A.E. studies give the sensitivity of A.E. systems to a reference source (at the site of the real source). The recommended reference source is the Nielsen pencil lead break. * (It is asked that this sensitivity is reported, where practicable, as an addition to any alternative normally used by the investigator).*

This calibration method was developed through experimentation by Arved Nielsen as described in the report: "Acoustic Emission Source Based on Pencil Lead Breaking", Report 80.15 which is available from the Danish Welding Institute, Park Allé 345, DK-2600 Glostrup, Denmark. A condensed review of this report is given in the following:

Introduction
Having recognised the necessity for a common reference AE signal, different methods have been investigated. Breaking a pencil lead on a structure surface has proved to be a suitable method; a simple device was developed and a paper presented at an EWGAE meeting in Rome, Sept. 1977.

The pencil is a commercial 0,5 mm lead type with a 4 mm fixed guide tube on which a PTFE ring is mounted as shown in Fig. C1. This ensures that the

* 2H Pentel, 3 mm length, 0,5 mm diam., with teflon guide ring.

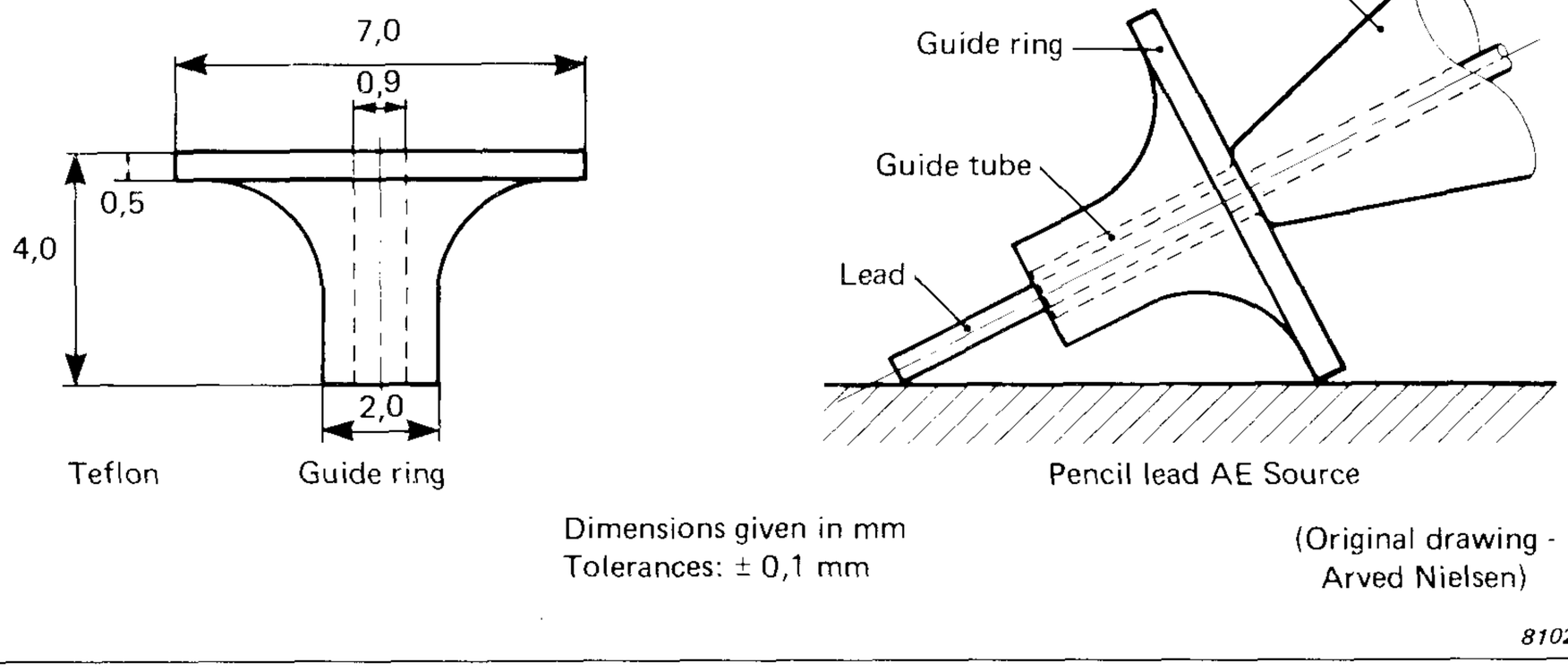

Fig. C1. The Nielsen reference source showing the teflon guide ring and the pencil position on a structure surface just before the lead is broken

breaking angle is constant and prevents spurious signals which occur if the guide tube touches the structure surface. *

The recommended application procedure is as follows:

1. The lead feed button on the pencil is pressed repeatedly until the lead protrudes.
2. The end of the lead is levelled with the end of the guide tube by pressing the tip of the pencil perpendicularly towards an even surface while the feed button is pressed down.
3. The button is pressed 6 times causing the lead to protrude 3 mm.
4. The pencil is guided obliquely towards the structure until the guide ring rests on the surface.
5. The pencil is pivoted about the point of contact towards a steeper position thus causing the lead to break.

Note: The pencil lead may be crushed in the guide tube resulting in acoustic signals which differ considerably in appearance from the normal signals. It is easy to observe such crushing by the reaction of the pencil when the lead is broken and acoustic signals from such events should be disregarded.

Experiments

In order to investigate the repeatability of this AE source an experimental method was established using the instrumentation shown in Fig. C2. The measurements were carried out by L. Hoff Hansen at Risø National Laboratory, Denmark.

* Replicas of the Nielsen reference source are available from B & K (order no. UA 0663).

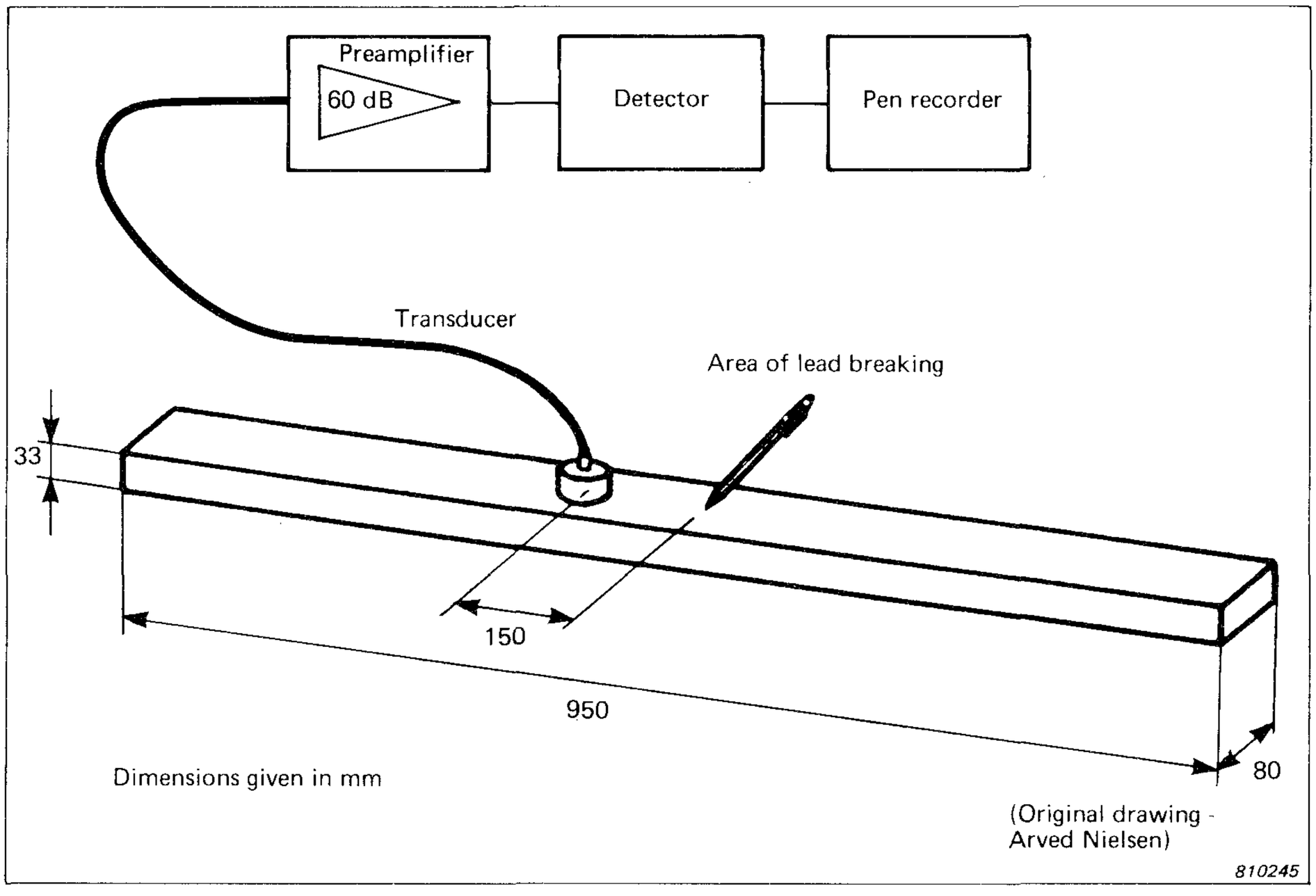

Fig. C2. Measurement of repeatability of the pencil lead break AE source

A commercial transducer is magnetically fixed to the ground surface of a steel bar and the pencil lead is broken on the surface at a distance of approximately 150 mm from the transducer. After an initial amplification of 60 dB, the numerical time integral of each detected signal is generated. The integrated signal, which has a decay time constant of 0,1 s (100 ms to e^{-1}, 230 ms for 20 dB decay), is then recorded as a single line on a pen recorder, the length of the line being proportional to the logarithm of the integrated AE signal.

During the experiments 10 identical pencils were used. Plastbound leads were used with hardness levels of 2H, 3H, 4H, 5H, and 6H.

Results

The following conclusions are made:

1. More than a couple of thousand observations result in a relative standard deviation in groups of about 100 events of 3 to 4 %.
2. The hardness of the lead had no significant influence on the magnitude of the generated AE signal. Other types of pencil leads may act differently.

3. It is convenient to standardize 6 steps in forwarding the pencil lead before the breaking process. If another number is used, both the protruding length of lead and the angle between the lead and the steel surface is changed, although little effect is observed on the magnitude of the AE signal.
4. The recorded signals correspond to AE peak signal amplitudes of about 4 mV referred to the transducer output. The preamplifier input noise level is 3 μV rms. The AE signals are, therefore, 60 dB higher than the rms noise (this has to be referred to the particular experimental conditions). When applied to steel structures a lower efficiency has to be expected.
5. The amplitude of the detected signal is approximately linearly related to the AE signal amplitude. However, the decay time of the detector is 100 ms and the penrecorder takes 1 s to reach 90 % full scale deflection, thus causing nonlinearity between the amplitudes of the detected signal and the penrecording. This is convenient for practical applications as the large range of signal amplitudes is compressed on the penrecordings, but the standard deviation indicated may be slightly misleading. On the basis of a linear relationship a factor of approximately 2 should be added, increasing the relative standard deviation to 7-10 %. (This is of the same magnitude as the relative standard deviation of 6,3 % in the 1,6 N load required to fracture the pencil lead which has been measured in other experiments.) A standard deviation of 10 % is by no means negligible; it implies that in 1 of 20 identical experiments the result will be more than 20 % from the average. This is not suitable for transducer calibration, but to control the operation of AE instrumentation on a steel structure the pencil lead source is very convenient. It is very helpful to repeat the lead breaking process, e.g. 5 times, to reduce the standard deviation of the average to half the standard deviation of single break.

Application of the Pencil Lead Source

Since its introduction the lead source has been used extensively in applications of the AE technique within the industry.

In a particular application the propagation of AE signals in pressure vessels and the influence of material type and experimental conditions were investigated. The pressure vessels were 0,5 m in diameter and 1,3 m in length.

The experiments resulted in relative standard deviations distributed over a wide range from 2 % to 16 % with an average of 5 %. This value is the standard deviation of an average of 10 observations; consequently the standard deviation of a single observation is about 15 %.

The value of 15 % is higher than the standard deviation of 7-10 % estimated from the experiments on the small steel specimen mentioned previously. The results obtained from the pressure vessels under various experimental conditions indicate that the type of experiment itself influences the resulting standard deviation.

In this discussion the detector output peak voltage has been considered. This represents the time integral of the AE signal. When the peak voltage of the AE signal was measured, the standard deviation was found to be approximately twice that obtained from the time integral of similar AE signals.

Acknowledgement

We would like to thank Mr. Arved Nielsen from the Danish Welding Institute for permission to publish material from his report and Mr. J. C. Hansen and Mr. T. Licht for editing the article.

News from the Factory

Measuring Amplifier Type 2636

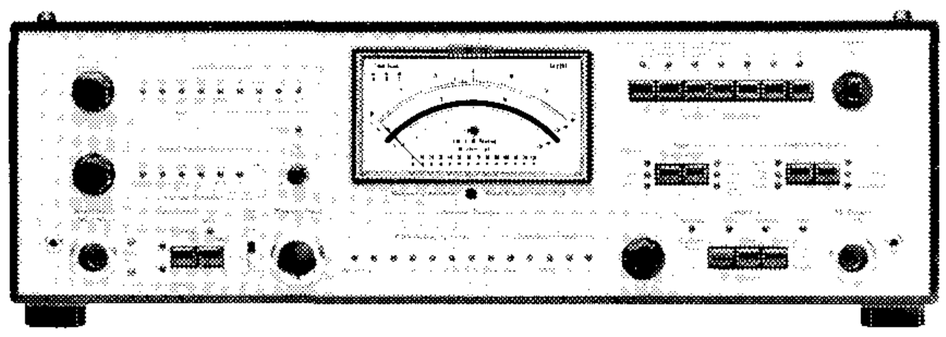

The B & K Measuring Amplifier Type 2636 is an easy to use calibrated amplifier-voltmeter having measuring ranges from 10 μV to 300 V FSD. It contains all the features of the Measuring Amplifier Type 2610, plus a variety of extra facilities. These greatly expand its useful range of applications in measurement and analysis set-ups for investigation of sound, vibration and voltage signals.

When used together with a half-inch B & K Condenser Microphone and preamplifier, it serves as an impulse precision sound level meter conforming to IEC 651 (Type 0), DIN 45 633 (part 1) and ANSI S1.4-1971 (Type 1) standards. It has a linear frequency range from 1 Hz to 200 kHz, built-in "A", "B", "C" and "D" weighting networks, and a 22,4 Hz high pass and a 22,4 kHz low pass filter.

For RMS measurements its Log Rectifier has a dynamic range of 70 dB and ± 0,5 dB overall (± 0,2 typical) indication accuracy for signals with crest factors up to 10 (up to 50 with reduced meter deflections). In addition to "Fast", "Slow" and "Impulse" time weighting functions, six averaging times between 0,1 and 30 s can be selected manually or remotely via the Averaging Time or Digital Interface sockets on the rear panel.

For comprehensive measurement of peak levels, "+ Peak", "– Peak" and "Max. Peak" indicating modes are available. To accommodate for different types of signal, independent selection of 5, 0,5 and 0,05 dB/μs rise rates plus "Fast", "Slow" and "0,5 s Hold" decay functions is possible. A separate

"Hold" mode permits the maximum Peak, RMS or Impulse level of short duration signals and single events to be captured and displayed.

For feeding magnetic tape as well as level and X—Y recording equipment there are two AC and one DC calibrated signal outputs from the Amplifier. Supplementing the analog outputs of the Amplifier is a Digital Interface bus conforming with IEC 625-1 for programmable measuring apparatus, and is for output of measurement data transmitted via a 10 bit A/D Converter in the instrument. Besides output of results, information can be sent of which front panel control settings are selected. The 2636 may also be controlled remotely via a programmable desk top calculator. Control lights on the front panel show which control settings are chosen as well as the status of the IEC interface.

In addition to a special program for automatic operation with a Band Pass Filter Type 1617 a program is provided for automatic self test of the 2636. This provides a basic check out of most analog functions available with the front panel control switches, testing the attenuator and detector linearity, filter thruput and noise, as well as the detector time constants. If a fault is detected, a warning is provided and a print out of the fault can be obtained.

Other facilities included in the 2636 are: Interchangeable meter scales for sound, vibration and voltage measurement; Automatic LED indication of gain, measuring range, and overload conditions; Built-in reference signal source for calibration; plus Direct and Microphone inputs (with selectable polarization voltage).

PREVIOUSLY ISSUED NUMBERS OF BRÜEL & KJÆR TECHNICAL REVIEW

(Continued from cover page 2)

4-1975 On the Measurement of Frequency Response Functions.

3-1975 On the Averaging Time of RMS Measurements (continuation)

2-1975 On the Averaging Time of RMS Measurements.
Averaging Time of Level Recorder Type 2306 and "Fast" and "Slow" Response of Level Recorders 2305/06/07.

1-1975 Problems in Telephone Measurements.
Proposals for the Measurement of Loudness Ratings of Operator's Headsets.
Comparison of Results obtained by Subjective Measuring Methods.
Repeatabilities in Electro-Acoustic Measurements on Telephone Capsules.
Stable Subset Measurements with the 73D.
Vibration Testing of Telephone Equipment.

4-1974 Underwater Impulse-Measurements.
A Comparison of ISO and OSHA Noise Dose Measurements.
Sound Radiation from Loudspeaker System with the Symmetry of the Platonic Solids.

3-1974 On Signal/Noise Ratio of Tape Recorders.
On the Operating Performance of the Tape Recorder Type 7003 in a Vibrating Environment.

SPECIAL TECHNICAL LITERATURE

As shown on the back cover page, Brüel & Kjær publish a variety of technical literature which can be obtained from your local B & K representative.

The following literature is presently available:

Mechanical Vibration and Shock Measurements
(English, German, Russian)
Acoustic Noise Measurements (English), 3 edition
Acoustic Noise Measurements (Russian), 2 edition
Architectural Acoustics (English)
Strain Measurements (English, German, Russian)
Frequency Analysis (English)
Electroacoustic Measurements (English, German, French, Spanish)
Catalogs (several languages)
Product Data Sheets (English, German, French, Russian)

Furthermore, back copies of the Technical Review can be supplied as shown in the list above. Older issues may be obtained provided they are still in stock.

Printed in Denmark by Nærum Offset

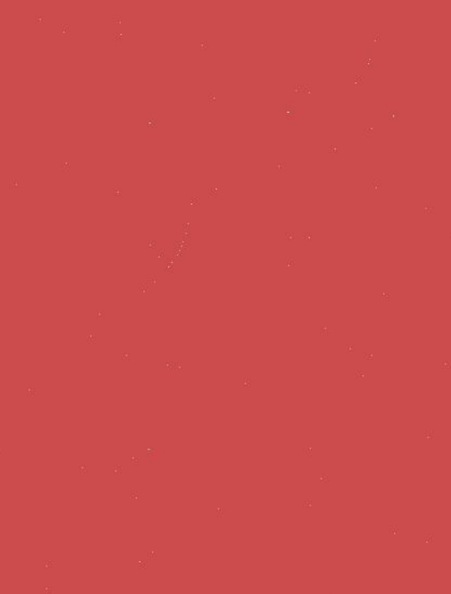

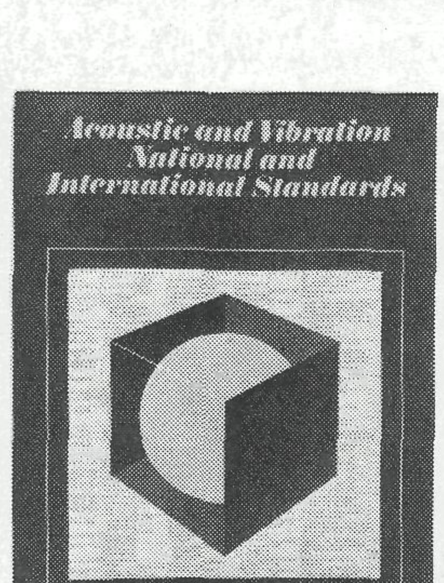

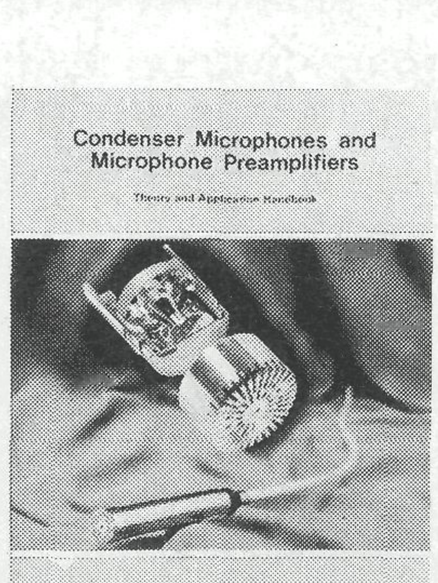

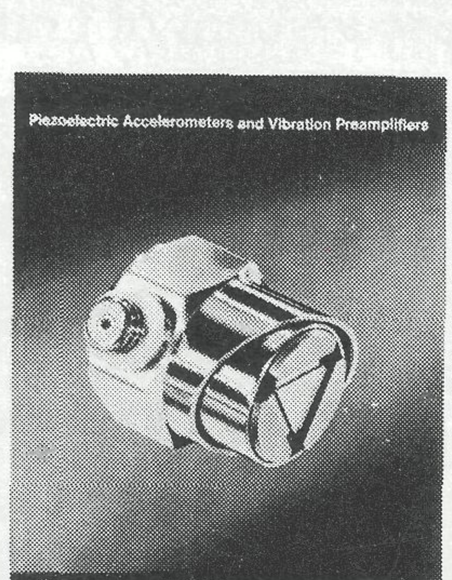

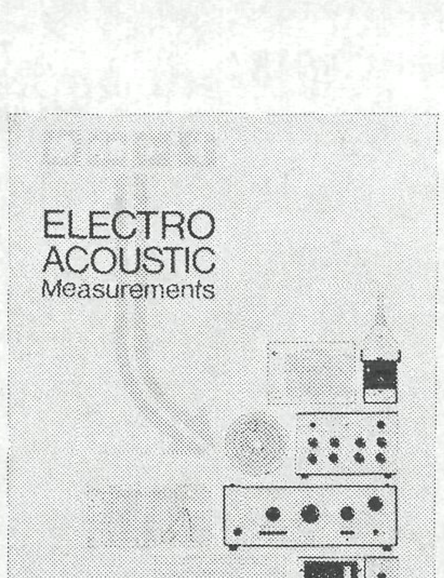

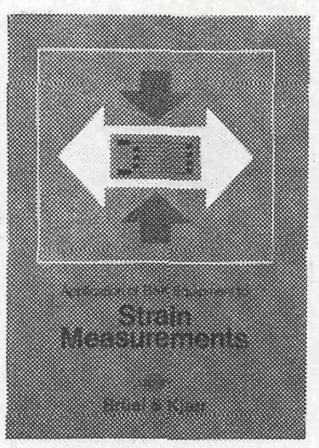

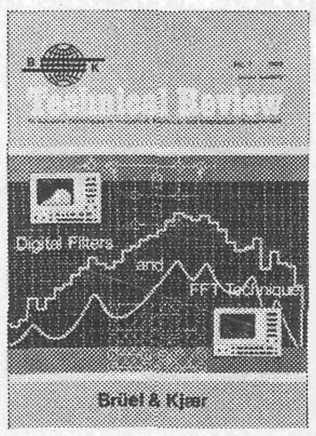

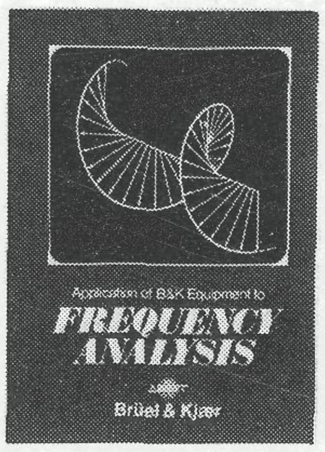

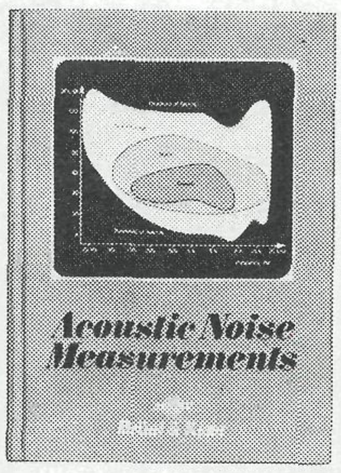

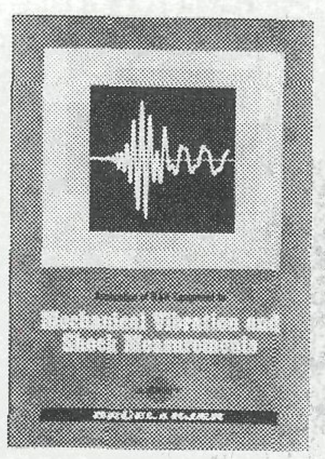

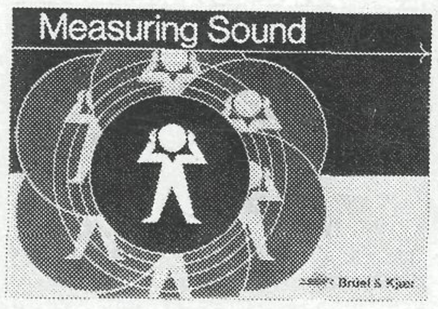

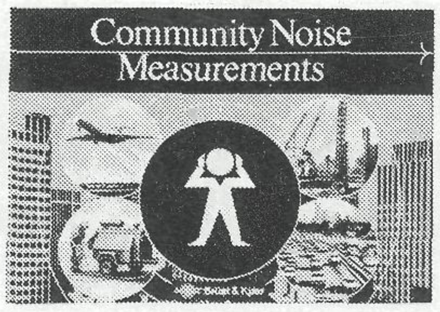

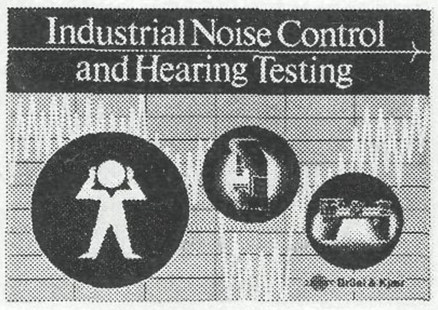

Brüel & Kjær

DK-2850 NÆRUM, DENMARK · Telephone: + 45 2 80 05 00 · Telex: 37316 bruka dk